UNIVERSIDAD DE CONCEPCIÓN
FACULTAD DE CIENCIAS FÍSICAS Y MATEMÁTICAS

PHASE TRANSITIONS AND BLACK HOLE STABILITY IN GAUGED $\mathcal{N} = 8$ SUPERGRAVITY

Por: Gabriel Ortega Gutiérrez

Tesis presentada a la Facultad de Ciencias Físicas y Matemáticas de la Universidad de Concepción para optar al grado académico de Magíster en Ciencias con Mención en Física

Junio 2026

Concepción, Chile

Profesor Guía: Dr. Andrés Anabalón Dupuy

A mis padres, mis hermanos y mi pareja.

AGRADECIMIENTOS

Quiero comenzar expresando mi gratitud a Juan Carlos López, mi profesor de Física en enseñanza media, quien fue el primero en creer en mis capacidades, confió en mí, nutrió mis habilidades y me impulsó a seguir este sueño. También doy las gracias al Dr. Andrés Anabalón, mi profesor guía durante el pregrado y el magíster, con quien me adentré en el estudio de la gravitación y la geometría. Valoro enormemente todo el apoyo que me ha brindado para ampliar mis horizontes mediante la participación en distintas instancias académicas de gran importancia. Del mismo modo, agradezco al Dr. Julio Oliva, profesor de quien he aprendido incontables tópicos valiosos y quien me impulsó a realizar lo que para mí parecía imposible, su carisma y paciencia hicieron de esta una experiencia inolvidable. Finalmente, extiendo mi gratitud al Dr. Guillermo Rubilar, quien comenzó siendo mi profesor en etapas tempranas de la carrera; con él aprendí grandes cosas que me acompañarán el resto de mi vida.

Valoro profundamente el apoyo incondicional de mi familia, sin ellos, nada de esto habría sido posible. Mi padre, Gabriel Agustín, mi madre, Marlene Sofía, y mis hermanos, Martín Agustín, Benjamín Santiago y María José, siempre me sacan una sonrisa, y disfruto su compañía más que nada. Ellos me entregaron los valores y principios con los que me guío, además de todo el cariño y respaldo que pude necesitar.

Deseo agradecer especialmente a mi pareja, Catherina Cabalín, quien ha sido mi apoyo incondicional, mi pilar fundamental y de quien he aprendido a amar por sobre todas las cosas. Haces que todo sea más fácil, siempre alegrando mis días. Gracias por tantos años de amor y por acompañarme en este largo proceso.

A la familia Cabalín Ferreira, quienes desde los primeros días me apreciaron y apoyaron como a un hijo más, siempre considerándome para todo. Bajo su techo pasé incontables tardes estudiando y trabajando. Para mí, ustedes también son familia.

A mi colega y amigo de la vida, Jorge Urbina, con quien las risas nunca faltan. Juntos hemos aprendido todo lo que sabemos, enseñándonos el uno al otro y

apoyandonos mutuamente en los peores momentos. Gracias por estar siempre ahí.

A mis amigos de la vida, con quienes he compartido el día a día o, a veces, instantes inolvidables, les agradezco su tiempo y su amistad sincera: Tomás Aguayo, Pablo Macchiavello, Agustín Saavedra, Efraín Orellana, Rogelio Muñoz, Eduardo Rivera, Daniel Vega, Julián Cantillana, Carlos Henríquez, Carlos Hormazábal, Juan José Avendaño, Tomás Durán y quizás algunos otros que se me quedan. Muchas gracias a todos.

Quisiera agradecer tambien al profesor Marcelo Oyarzo, quien en las últimas etapas de la carrera nos enseño muchísimo y que siempre tuvo la voluntad de ayudar, muchas gracias por todo.

Por último, pero no menos importante, agradezco a mi gata, Whisky, quien siempre me brindó su compañía en incontables noches de estudio. Le estaré agradecido por siempre por todo su amor y cariño sin límites.

El trabajo de esta tesis fue apoyado por el proyecto Fondecyt Regular 1250133 y por la Universidad de Concepción, gracias a su beca de arancel para posgrado.

Resumen

Esta tesis presenta un estudio termodinámico detallado de agujeros negros planares y solitones de Anti-de Sitter (AdS) en el marco del modelo STU en $D = 4$. Este se define como una truncación consistente de la teoría de supergravedad $\mathcal{N} = 8$ gaugeada, teoría que describe el sector sin masa de la compactificación de Kaluza-Klein de la supergravedad en once dimensiones sobre una siete-esfera (S^7). Finalmente, esta está identificada como el límite de bajas energías de la Teoría M. Específicamente, se explora la truncación T^3, donde, tras imponer una simetría específica sobre las cargas, la dinámica de los tres campos dilatónicos se simplifica en un único dilatón efectivo acoplado a dos cargas independientes. El foco de esta investigación es la completación del espacio de fases térmico para configuraciones foliadas con hipersuperficies de codimensión-2 con topología planar, en las cuales los solitones AdS emergen como los candidatos naturales a vacío de la teoría y actúan como el análogo gravitacional de la fase de confinamiento en la teoría dual. El análisis se desarrolla tanto en el ensamble microcanónico como en el gran canónico, permitiendo una descripción analítica de las transiciones entre las distintas configuraciones gravitacionales.

Un aporte fundamental y desafío técnico de este trabajo radica en el tratamiento de los múltiples campos de gauge y escalares propios de estas teorías, factores que complejizan significativamente el análisis termodinámico. Como resultado principal, se presenta un mapeo sistemático de las zonas de estabilidad en el espacio de parámetros del modelo, una tarea inédita que no ha sido documentada previamente en la literatura. Este mapeo permite una comprensión profunda de la estructura de fases de este sector de la supergravedad, llenando un vacío esencial en la descripción de estas soluciones.

Palabras Clave – Correspondencia AdS/CFT, Agujeros Negros en Teoría de Cuerdas, Solitones

Abstract

This thesis presents a detailed thermodynamic study of planar black holes and Anti de Sitter (AdS) solitons within the framework of the $D = 4$ STU model. This is defined as a consistent truncation of gauged $\mathcal{N} = 8$ supergravity, a theory that describes the massless sector of the Kaluza-Klein compactification of eleven dimensional supergravity on a seven sphere (S^7). Finally, this is identified as the low energy limit of M theory. Specifically, we explore the T^3 truncation where, after imposing a specific symmetry on the charges, the dynamics of the three dilatonic fields simplify into a single effective dilaton coupled to two independent charges. The focus of this research is the completion of the thermal phase space for configurations foliated with codimension two hypersurfaces of planar topology, in which AdS solitons emerge as natural vacuum candidates of the theory and act as the gravitational analog of the confining phase in the dual theory. The analysis is developed in both the microcanonical and grand canonical ensembles, allowing an analytical description of the transitions between different gravitational configurations.

A fundamental contribution and technical challenge of this work lies in the treatment of the multiple gauge and scalar fields inherent to these theories, factors that significantly complicate the thermodynamic analysis. As a main result, we present a systematic mapping of the stability regions within the parameter space of the model, an unprecedented achievement not previously documented in the literature. This mapping provides a profound understanding of the phase structure in this sector of supergravity, filling an essential gap in the description of these solutions.

Keywords – AdS/CFT Correspondence, Black Holes in String Theory, Solitons

Índice general

Índice de figuras

Capítulo 1

Introduction

The quest for a unified description of the fundamental forces of nature has remained the central ambition of theoretical physics for over a century. Our current understanding of the universe rests upon two seemingly irreconcilable pillars: the Standard Model of particle physics, which gives a consistent and predictive description of the quantum behavior of electromagnetic, weak, and strong interactions for energy scales up to the TeV ($\sim 10^3\, GeV$), and General Relativity, which describes gravity as the curvature of the space-time manifold. General Relativity has proven to be an exceptionally robust theory, passing fundamental tests such as the precise prediction of the perihelion precession of Mercury and the deflection of light by massive bodies. More recently, the direct detection of gravitational waves has provided a new window into the universe, confirming Einstein's predictions in extreme gravitational regimes. However, despite its triumphs, General Relativity remains a classical theory. When one attempts to quantize gravity using the same tools that were so successful for the Standard Model, the theory becomes non-renormalizable. At the Planck scale, characterized by length of $1{,}6 \times 10^{-35}$ m and energy scales of approximately $10^{19}\, GeV$, the classical description of space-time as a smooth Lorentzian manifold ceases to be valid. In this regime, the non-renormalizable nature of the Einstein-Hilbert action manifests as the breakdown of the perturbative expansion, where the coupling constant leads to uncontrollable divergences in the calculation of scattering amplitudes. Physically, this implies that at such scales, the gravitational back-reaction of any probe becomes comparable to the background geometry itself, rendering the distinction between a fixed background and quantum excitations

ill-defined. This fundamental conflict signals that General Relativity and the Standard Model must be viewed as effective descriptions of a more profound, ultraviolet-complete theory of Quantum Gravity.

To resolve the inconsistencies between these two theories, String Theory emerges as one of the most prominent candidates. Within this framework, the fundamental constituents are not zero-dimensional particles, but one-dimensional extended objects whose vibrational modes correspond to the particles observed in nature. A cornerstone of these theories is supersymmetry, a symmetry that relates bosons and fermions. A remarkable feature of this symmetry is that when it is promoted to a local symmetry, it naturally incorporates gravity, leading to the framework of supergravity. In this regime, specifically at energy scales E much smaller than the characteristic string scale M_s, the degrees of freedom associated with the massive excitations of the string are not accessible and can be formally integrated out. What remains is a massless effective field theory, the supergravity theory, which describes the dynamics of the graviton, its fermionic superpartners (the gravitinos), and a collection of gauge and scalar fields. These theories provide a concrete Lagrangian where the geometric and particle physics properties of the universe are unified under a single symmetry principle. However, a fundamental characteristic of string theories is that they intrinsically require ten or eleven spacetime dimensions to be mathematically consistent. To reconcile this higher dimensional geometry with our observable four dimensional universe, we postulate that these extra spatial directions are curled up into microscopic compact manifolds. Because these internal dimensions are extremely small, exciting any physical momentum modes along them requires an enormous amount of energy. Consequently, at low energy scales, these massive Kaluza-Klein modes decouple and the extra directions go effectively unnoticed, allowing us to describe the physics accurately through effective four dimensional theories.

The landscape of four-dimensional supergravity is diverse, as the specific form and content of each theory are restricted by the number of independent supersymmetries, denoted by $\mathcal{N}$, preserved by the vacuum. These are referred to as extended supergravities when $\mathcal{N} > 1$. As $\mathcal{N}$ increases, the theory becomes significantly more constrained. Among these, $\mathcal{N} = 8$ supergravity stands as a unique framework, representing the maximal supergravity theory possible in four dimensions. With 32 independent supercharges, it is the most symmetric

field theory that can be constructed without involving particles with spin higher than two, a limit beyond which consistent interacting field theories are generally believed to be impossible. This high degree of symmetry makes this theory remarkably predictive and has led to long-standing conjectures regarding its potential ultraviolet finiteness, positioning it as a leading candidate for a consistent quantum field theory of gravity. Furthermore, as the four-dimensional manifestation of eleven-dimensional supergravity compactified on a seven-sphere (S^7), it serves as the primary arena for exploring the low-energy dynamics of M-theory.

Within these theories, a critical distinction exists between ungauged and gauged supergravities. In ungauged supergravities, the "R-symmetry", which rotates the supercharges of the theory, is a global symmetry. However, in gauged supergravities, this R-symmetry is made local, or "gauged", which requires the introduction of gauge fields. This process of gauging is not merely a formal exercise, it naturally generates a non-trivial potential for the scalar fields of the theory. This potential typically acts as a negative cosmological constant, giving rise to vacua that are asymptotically Anti-de Sitter. The study of AdS spaces is fundamental due to the AdS/CFT correspondence [1–4], which states a duality between gravity in a d-dimensional bulk and a conformal field theory on its $(d-1)$-dimensional boundary. Under this mapping, black holes in the bulk represent thermal states in the dual theory [5]. Specifically, this thesis focuses on planar black holes, where the topology of the event horizon is that of a plane. These black holes are of vital importance in holography because they allow for the study of field theories defined on flat space, providing a direct link to the physics of the quark-gluon plasma and condensed matter systems [6].

In the study of black hole thermodynamics within AdS, a celebrated phenomenon is the Hawking-Page transition [7], which describes a phase transition between thermal AdS and a large stable Schwarzschild-AdS black hole. This phase transition is fundamental for describing the onset of confinement in the dual field theory and serves as a benchmark for studying more complicated phenomena. While this transition is fundamental for spherical topologies, it does not take place in planar topologies. In this case, the black hole remains the globally preferred state over thermal AdS for all temperatures $T > 0$, as its free energy is always lower than that of the thermal AdS. This persistent dominance would seemingly suggest a lack of interesting phase structure. However, it is essential to distinguish

between global thermodynamic preference and local stability. A configuration that possesses a lower free energy than a thermal gas may still be locally unstable, for example, by exhibiting a negative specific heat, meaning it cannot represent a physically realized equilibrium state.

From a holographic perspective, it is natural to seek a vacuum state that can adequately represent the confinement phase of the dual field theory. In planar topologies, this role is uniquely filled by the AdS Soliton. The competition between the planar black hole and the AdS Soliton thus restores the rich phase structure expected from a holographic model, see [8–12].

In theories with a sophisticated field content, such as gauged $\mathcal{N} = 8$ supergravity, this competition is fundamentally shaped by the presence of multiple gauge charges and dilatonic fields. This maximal theory provides a crucial low-energy effective description of the parent theory's physics post-compactification. The STU model, as a consistent truncation of this theory, retains four independent $U(1)$ gauge charges, making it a key framework for investigating how the interplay of multiple charges influences the thermodynamic phase structure. The combination of these diverse gauge fields and the non-trivial scalar sector transforms the search for stable regions into a complex multidimensional challenge, as configurations must be analyzed across a broad parameter space. Moreover, it is known that there is a region of the parameter space where static dilatonic black holes are never locally stable within the STU models of the maximal gauged supergravities [13–17]. Achieving a complete understanding of the fate of these thermal states through holography remains an important open problem; for recent work, see [18–27]. Recently, a new family of supersymmetric solitons has been shown to exist within different truncations of the STU models of maximal gauged supergravities [28–32]. These geometries generalize the AdS soliton geometry found in [33]. They are horizonless geometries that are well-suited to describe holographic confinement; for recent works, see [34–46, 46–51]. Hence, it is of interest to investigate how these geometries fit into the phenomenology of maximal supergravities. In particular, this thesis shows that they provide the natural competing saddles for the electrically charged black holes discussed above, and identifies when the corresponding first-order transition preempts the local instability.

This thesis addresses this challenge by providing an unprecedented mapping of these stability zones in both the microcanonical and grand canonical ensembles

for planar configurations, a task that, despite the maturity of the STU model, has not been previously documented in the literature.

This thesis is organized as follows:

In Chapter 2: Theoretical Framework we establish the foundational physics of the study, beginning with the origin of the STU model as a consistent truncation of eleven-dimensional supergravity, the low-energy limit of M-theory. It explains the process of reduction to four-dimensional $SO(8)$-gauged $\mathcal{N} = 8$ supergravity and the subsequent simplification to the T^3 sector. This chapter also provides a rigorous analysis of scalar fields in Anti-de Sitter space, specifically the Breitenlohner-Freedman bound, and introduces the geometric structures of both planar black holes and AdS solitons. Central to this framework is the review of the Hawking-Page transition, analyzed as a fundamental benchmark for describing the confinement-deconfinement phase transition in the dual field theory. Special emphasis is placed on the planar limit, where the absence of the standard Hawking-Page transition necessitates the introduction of the AdS soliton to restore the rich phase structure expected from a holographic model. Finally, we review the principles of black hole thermodynamics, distinguishing between local stability, governed by the Hessian of the energy, and global stability, evaluated through free energy competition.

In Chapter 3: Thermodynamics of Planar Black Holes in the STU Model, we present the core analytical results regarding the stability of the system. It derives the exact, analytical equation of state in the microcanonical ensemble. From this, the 5×5 Hessian matrix is computed to identify the precise charge ratios that bound the region of local stability for the T^3 model. These microcanonical boundaries are then systematically mapped into the grand canonical ensemble using Legendre transformations, providing a clear characterization of the stable thermal states and their free energy densities.

In Chapter 4: First Order Phase Transition, we investigate the global thermodynamic competition between the planar black hole and the AdS soliton. The chapter derives the coexistence condition between both saddles and introduces a critical compactification scale that determines when the solitonic first-order transition occurs before the black hole reaches its local instability. This provides a refined characterization of the range of boundary compactifications where the soliton preempts the spinodal region.

In Chapter 5: Conclusions, we summarize the primary findings of the research, reflecting on the role of multiple gauge charges, dilatonic fields, and compactification scales in creating complex phase structures. It highlights the role of the critical scale that separates compactifications where the solitonic transition preempts the local instability from those where additional physics may be required.

Capítulo 2

Theoretical Framework

2.1. The STU Model: From M-Theory to 4D Physics

The theoretical foundation of this work is rooted in eleven-dimensional supergravity [52], which is widely recognized as the low-energy limit of M-theory [53]. The field content of $11D$ supergravity consists of a single supermultiplet that contains the eleven-dimensional metric G_{MN}, a 3-form gauge field A_{MNP}, and a 32-component Majorana spinor known as the gravitino Ψ_M. A known result is that this theory can be reduced to four dimensions by considering a Kaluza-Klein reduction on a deform seven-sphere (S^7), a space-time of the form $AdS_4 \times S^7$ [54]. In this setup, the effective 4D physics is described by the $\mathcal{N} = 8$ gauged supergravity, where the gauge group $SO(8)$ arises naturally from the isometries of the internal seven-sphere [55], often called SO(8)-gauged $\mathcal{N} = 8$ supergravity.

While the 11D theory is relatively simple, the resulting four-dimensional $\mathcal{N} = 8$ supergravity theory is remarkably complex. Its field content consists of a single gravitational multiplet: the graviton $g_{\mu\nu}$, 8 spin-3/2 gravitini ψ_μ^I transforming in the fundamental representation of $SO(8)$, 28 vector fields A_μ^{IJ}, 56 spin-1/2 fermions χ^{IJK}, and 70 scalar fields Φ^{IJKL}. This collection of 128 bosonic and 128 fermionic degrees of freedom represents the most symmetric field theory constructible in four dimensions without involving particles of spin higher than two. However, the huge number of interacting fields makes the task of finding exact, non-trivial analytic solutions practically impossible.

To make the problem treatable, we employ the technique of considering a consistent truncation. This means, finding a subset of fields such that they can be set to zero without imposing any constrains on the remaining not-truncated fields, and that every truncated field satisfy their own equation of motion identically. In this work, the first step of the truncation involves the fermionic sector. Since we are interested in purely bosonic backgrounds, such as classical black holes and solitons, we set all fermionic fields (gravitinos and spin-1/2 fermions) to zero.

The STU model is a specific consistent truncation of the maximal theory that further simplifies the bosonic sector by focusing on the Abelian part of the theory, by retaining only the singlets under the $SO(2) \times SO(2) \times SO(2)$ diagonal inside the $SO(8)$, the theory reduces to a model containing the graviton, four $U(1)$ gauge fields (A^i_μ), and three complex scalar fields (z_1, z_2, z_3), commonly referred to as s, t, and u, where the name of the model comes from. These complex scalars parameterize the coset space $[SL(2,\mathbb{R})/SO(2)]^3$. Each complex field z_i can be decomposed into two real degrees of freedom: a dilaton Φ_i and an axion χ_i, typically written as $z_i = \chi_i + ie^{-\Phi_i}$.

For the purposes of this thesis, we further restrict our analysis to the purely dilatonic sector of the STU model. This is achieved by another truncation, where all three axions are set to zero ($\chi_1 = \chi_2 = \chi_3 = 0$).We will consider either purely magnetic or purely electric solutions, so it is consistent to truncate the axions to zero in this sector. This leaves us with a theory of gravity coupled to four gauge fields and three real dilatons. Under these truncation conditions, the action of the STU model on the bulk takes the following form

$$\mathcal{S} = \frac{1}{2\,\kappa} \int d^4x\, \sqrt{-g} \left(R + \sum_{a=1}^{3} \left[-\frac{(\partial \Phi_a)^2}{2} + \frac{2}{L^2}\, \cosh\left(\Phi_a\right) \right] - \frac{1}{4} \sum_{\Lambda=1}^{4} X_\Lambda^{-2} F_\Lambda^2 \right) , \tag{2.1.1}$$

where

$$F_\Lambda = dA_\Lambda\,, \qquad X_\Lambda = e^{-\frac{1}{2}\vec{a}_\Lambda \cdot \vec{\Phi}}\,, \qquad \vec{\Phi} = (\Phi_1, \Phi_2, \Phi_3)\ , \tag{2.1.2}$$

and

$$\vec{a}_1 = (1,1,1)\,, \qquad \vec{a}_2 = (1,-1,-1)\,, \qquad \vec{a}_3 = (-1,1,-1)\,, \qquad \vec{a}_4 = (-1,-1,1)\,. \tag{2.1.3}$$

In our conventions, $\kappa = 8\pi G$ (with G being the four-dimensional Newton constant) and L represents the AdS radius.

An explicit uplift of this sector of the theory to $11D$ supergravity can be found in [56]. Finally, it is possible to further truncate the STU model into simpler single-scalar sectors by imposing specific identification symmetries among the four Abelian gauge charges Q_I. These reductions lead to the so-called T and T^3 models, which are defined by the following configurations:

- The T Model: Defined by the pairwise identification of charges, $Q_1 = Q_2$ and $Q_3 = Q_4$. This choice consistently truncates the scalar manifold such that $\Phi_1 = \Phi_2 = 0$, leaving a single active dilaton field.
- The T^3 Model: Defined by the identification of three of the gauge charges, $Q_2 = Q_3 = Q_4$. This symmetry identifies the three dilatonic fields, $\Phi_1 = \Phi_2 = \Phi_3 = \Phi$, effectively collapsing the dynamics into an effective single-dilaton theory coupled to two independent gauge fields.

These models are particularly relevant as they retain the non-linear structure of the original theory while providing a more tractable framework for studying the thermodynamic phase space and the stability of the solutions. In this work we focus only on the T^3 model.

Consistent Truncation: To clarify this concept, let us consider a toy model with two degrees of freedom described by the following Lagrangian:

$$L(q_1, q_2) = \frac{1}{2}\dot{q}_1^2 + \frac{1}{2}\dot{q}_2^2 - q_1 q_2^2. \tag{2.1.4}$$

The resulting equations of motion are:

$$\ddot{q}_1 + q_2^2 = 0, \tag{2.1.5}$$

$$\ddot{q}_2 + 2q_1 q_2 = 0. \tag{2.1.6}$$

Suppose we seek solutions where the first field vanishes, i.e., we propose the reduced ansatz $q_1(t) = 0$. Substituting this into (2.1.5), we find that $q_2(t)$ is forced to be zero. In this case, the ansatz is overly restrictive, and the only solution allowed by the full dynamics is the trivial one, $q_1 = q_2 = 0$.
However, a conflict arises if we perform the truncation at the level of the action. If we set $q_1 = 0$ in the Lagrangian (2.1.4) *before* varying the fields, we obtain:

$$L_{\text{red}}(q_2) = \frac{1}{2}\dot{q}_2^2, \tag{2.1.7}$$

which yields the reduced equation of motion:

$$\ddot{q}_2 = 0. \tag{2.1.8}$$

This reduced equation allows for non-trivial solutions, which clearly do not satisfy the original system (2.1.5)-(2.1.6).
Therefore, truncating degrees of freedom in the Lagrangian is not generally equivalent to truncating them in the equations of motion. A truncation is called **consistent** only if every solution of the reduced theory is also a solution of the full theory. Mathematically, this failure occurs whenever the truncated field (q_1) appears linearly in the interaction terms of the Lagrangian, as it acts as a source for the remaining fields (q_2), preventing them from evolving independently.

2.1.1. Black Holes and Solitons in the STU Model

The STU model is well-known for admitting a wide variety of solutions, ranging from rotating and magnetic black holes to more complicated dyonic configurations [13, 56, 57]. To provide a clear investigation of thermodynamic stability and phase transitions, this work focuses on the static and purely electric sector. This choice allows for a analytic analysis of the parameter space without the added complications introduced by rotation or magnetic charges.

The four-charge electric black hole in the dilatonic sector of the STU model, with a spherical horizon, was found in [13], and its generalizations to planar and hyperbolic horizons were constructed in [56]. Here, we present the solution for arbitrary horizon geometry controlled by the parameter $k = -1, 0, 1$ leading to hyperbolic, planar and spherical horizons respectively. The explicit form of the metric, in the coordinates of [21] is

$$\begin{aligned} ds^2 &= -\frac{f(r)}{\sqrt{H(r)}}dt^2 + \frac{\sqrt{H(r)}}{f(r)}dr^2 + r^2\sqrt{H(r)}\left(\frac{dx^2}{1-kx^2} + \left(1-kx^2\right)d\varphi^2\right), \\ f(r) &= k + \frac{r^2}{L^2}H(r) - \frac{m}{r} - \frac{q}{r^2}, \quad H(r) = H_1H_2H_3H_4, \quad H_\Lambda = 1 + \frac{q_\Lambda}{r}. \end{aligned} \tag{2.1.9}$$

The coordinate φ labels a flat coordinate, which could be either compact or non-compact. The dilatons and the gauge fields are

$$\begin{aligned} &\Phi_1 = \frac{1}{2}\log\left(\frac{H_2H_3}{H_1H_4}\right), \quad \Phi_2 = \frac{1}{2}\log\left(\frac{H_1H_3}{H_2H_4}\right), \quad \Phi_3 = \frac{1}{2}\log\left(\frac{H_1H_2}{H_3H_4}\right), \\ &A^\Lambda = \left(\frac{Q_\Lambda}{rH_\Lambda} - \mu_\Lambda\right)\mathrm{d}t, \quad Q_\Lambda^2 = q_\Lambda^2 k + q_\Lambda m - q. \end{aligned} \tag{2.1.10}$$

This configurations are characterized by a set of parameters fundamentally related to the physical observables of the system. Specifically, m is an integration constant related to the physical mass M through the general relation $M \propto m + \frac{k}{2}\sum q_\Lambda$, and the quantities Q_Λ are proportional to the physical electric charges of the gauge fields. The parameters q_Λ characterize the scalar hair, controlling the profile of the dilatonic fields relative to the AdS vacuum. The quantity q is a parameter

introduced through a diffeomorphism, a shift of the radial coordinate, which allows a simple limit to the BPS configuration. Finally, the constants μ_Λ are the chemical potentials which are fixed so that the gauge fields are regular in the Euclidean continuation.

In this work we will focus on black holes with planar horizons, thus, we will consider the metric (2.1.9) with $k = 0$.

Another class of solutions for the metric in Anti-de Sitter space has been shown to exist, which exhibit a remarkably different topological structure compared to black holes: the AdS solitons. Historically, these configurations were introduced by Horowitz and Myers as the gravitational ground state for theories where one of the spacelike planar directions of the conformal boundary is compactified.

Physically, the AdS soliton represents a "cigar-like" geometry where a spatial dimension closes off at a finite radius, effectively capping the space-time before a singularity or horizon can form. It is important to note that these solitons exist only for the planar topology. Within this framework, the soliton metric is not an independent construction but is intimately related to the black hole solution. Specifically, these configurations are obtained via a double analytic continuation of the coordinates by means of a double Wick rotation of the time coordinate and one of the cyclic coordinates,

$$t \to i\varphi, \quad \varphi \to it. \tag{2.1.11}$$

In this way, the black hole's event horizon is transformed into the "tip" of the soliton's geometry. As a consequence of this, the one-form dt has always a negative norm. Thus, time remains a globally defined coordinate throughout the manifold.

In the solution presented in (2.1.10), the double Wick rotation (2.1.11) must be accompanied by an analytic continuation of the gauge-field parameters. Indeed, since the black hole gauge potentials are proportional to dt, the replacement $t \to i\varphi$ would make them imaginary if the electric charges and chemical potentials were kept real. To obtain a real solitonic configuration, one must take

$$Q_\Lambda \to i\widetilde{Q}_\Lambda, \qquad \mu_\Lambda \to i\widetilde{\mu}_\Lambda. \tag{2.1.12}$$

After this continuation, the gauge field is supported along the compact direction φ.

Therefore, A_φ is no longer interpreted as an electric potential, rather, it represents a magnetic flux, or equivalently a Wilson line, around the compact circle.

Because of this specific topological arrangement, if the metric of the conformal boundary has a compact direction $\varphi \in [0, \Delta]$, then, in principle, it is possible to construct a soliton with these boundary conditions. The fact that the time coordinate is globally defined, allows the soliton to exist with arbitrary chemical potentials. This must be contrasted with the black hole case, in which there is a horizon which requires to impose regularity constraints that typically tie the gauge fields to the temperature. This makes the soliton the natural candidate for the vacuum state of the theory in the planar case, providing a structural alternative to the standard black hole geometry.

2.1.2. Scalar Fields in Anti-de Sitter Space and the BF Bound

To fully understand the thermodynamic behavior of the STU model and its holographic implications, it is necessary to analyze the fundamental properties of its scalar sector. In flat spacetime, a scalar field with a negative mass squared implies the existence of tachyonic modes, leading to a vacuum instability. However, in Anti-de Sitter spacetime, the geometry itself acts as an effective confining potential well. This geometrical feature allows scalar fields to possess a negative mass squared without destabilizing the vacuum, provided this mass satisfies a strict lower limit known as the Breitenlohner-Freedman (BF) bound [58].

In the context of holography, we are primarily concerned with the asymptotic behavior of the spacetime as the radial coordinate approaches infinity. To preserve the asymptotic AdS symmetries at the conformal boundary, any regular scalar field must vanish in this limit ($\Phi \to 0$). Therefore, strictly near the boundary, the scalar field is infinitesimally small, and higher-order non-linear interactions become completely negligible. In this asymptotic regime, the scalar field must behave exactly like a free field whose dynamics are entirely governed by its effective perturbative mass around the vacuum.

This perturbative mass is extracted by expanding the scalar potential $U(\Phi)$ around the critical point $\Phi = 0$ up to quadratic order. It is important to note that, for this potential, $\Phi = 0$ corresponds to a local maximum. Consequently, mapping the

coefficient of the quadratic term to a standard real scalar field mass term, $\frac{1}{2}m^2\Phi^2$, yields a negative mass squared ($m^2 < 0$). The physical viability and stability of this configuration will be addressed in this section.

The mass of the scalar field rigidly determines its asymptotic fall-off profile. This can be proven by solving the Klein-Gordon equation, $\Box\Phi - m^2\Phi = 0$, we will do this in the asymptotic limit of the planar black hole. In the boundary, the planar geometry reduces to the pure AdS_4 Poincaré patch, this is

$$ds^2 \approx -\frac{r^2}{L^2}dt^2 + \frac{L^2}{r^2}dr^2 + r^2(dx^2 + dy^2). \tag{2.1.13}$$

Were L denotes the AdS radius. Then, assuming a planar-symmetric (which does not depend on the (x, y) coordinates) and static scalar field that depends only on the radial coordinate, $\Phi = \Phi(r)$, in the coordinates of (2.1.13) the d'Alembertian operator simplifies to

$$\Box\Phi = \frac{1}{\sqrt{-g}}\partial_r\left(\sqrt{-g}g^{rr}\partial_r\Phi\right) = \frac{1}{r^2}\partial_r\left(r^2\left(\frac{r^2}{L^2}\right)\partial_r\Phi\right). \tag{2.1.14}$$

Evaluating the derivative yields

$$\Box\Phi = \frac{r^2}{L^2}\Phi'' + \frac{4r}{L^2}\Phi'. \tag{2.1.15}$$

Substituting this back into the Klein-Gordon equation and multiplying by L^2/r^2, we obtain a homogenous Euler-Cauchy differential equation

$$r^2\Phi'' + 4r\Phi' - m^2L^2\Phi = 0. \tag{2.1.16}$$

Then, we impose a power-ansatz $\Phi(r) = r^{-\Delta}$, as it is known that this are solutions to this kind to the Euler-Cauchy equation. Substituting this anzats into (2.1.16), we get

$$\Delta(\Delta + 1) - 4\Delta - m^2L^2 = 0 \implies \Delta^2 - 3\Delta - m^2L^2 = 0. \tag{2.1.17}$$

Using the quadratic formula, we find the two values of Δ that dictate the radial

fall-off of the scalar field

$$\Delta_{\pm} = \frac{3}{2} \pm \sqrt{\frac{9}{4} + m^2 L^2}. \tag{2.1.18}$$

This exact result reveals the physical origin of the Breitenlohner-Freedman bound. For the scalar field to be physically well-behaved at infinity [1], the roots $\Delta_{\pm}$ must be strictly real numbers. This imposes that the argument of the square root must be non-negative

$$\frac{9}{4} + m^2 L^2 \geq 0 \implies m^2 \geq -\frac{9}{4L^2} = m^2_{\text{BF}}. \tag{2.1.19}$$

This way, we get that, in four dimensions, the Breitenlohner-Freedman bound is given by $m^2_{\text{BF}} = -9/4L^2$, which allows the existence of stable scalar fields with a negative squared mass as long as $m^2 \geq m^2_{\text{BF}}$ propagating in the Anti de Sitter spacetime. As long as this bound is satisfied, the field decays smoothly towards the boundary as

$$\Phi(r) \approx \frac{\alpha}{r^{\Delta_-}} + \frac{\beta}{r^{\Delta_+}}. \tag{2.1.20}$$

Scalar Fields in the STU Model:

We can now apply this framework to the dilatons in the STU model. As defined in (2.1.1), the relevant bosonic Lagrangian density for our theory is

$$\mathcal{L}_{\text{bosonic}} = \sum_{a=1}^{3} \left[-\frac{(\partial \Phi_a)^2}{2} + \frac{2}{L^2} \cosh(\Phi_a) \right] - \frac{1}{4} \sum_{\Lambda=1}^{4} X_{\Lambda}^{-2} F_{\Lambda}^2. \tag{2.1.21}$$

where the scalar fields are non-trivially coupled to the Abelian gauge fields through the exponential factors $X_{\Lambda}(\vec{\Phi})$.

At first sight, one might assume that this direct dilatonic coupling to the Maxwell fields complicates the extraction of the mass of the scalar fields. However, in classical field theory, the fundamental parameters of a model, such as the cosmological constant and the masses of the fields are intrinsic properties of the background spacetime itself, independent of any specific solution.

[1] meaning it does not develop complex, runaway oscillating modes.

To extract the mass of the dilatons, we must evaluate their dynamics strictly in the ground state of the theory, this is the pure, empty AdS vacuum. In this foundational state, there are no macroscopic black holes and no background electromagnetic fluxes. Therefore, the Maxwell fields are identically zero ($F_\Lambda \equiv 0$). The charged planar black holes we study are simply classical excitations built on top of this background.

Because the fundamental mass is determined by the background vacuum, the coupling term vanishes entirely, and the perturbative dynamics of the dilatons are dictated exclusively by the isolated scalar potential

$$U(\vec{\Phi}) = -\sum_{a=1}^{3} \frac{2}{L^2} \cosh(\Phi_a). \tag{2.1.22}$$

Because there are no cross-terms coupling the different dilatons to one another in this potential, the mass matrix is completely diagonal. Expanding this potential around the vacuum $\Phi_a = 0$ up to quadratic order yields

$$U(\vec{\Phi}) = -\sum_{a=1}^{3} \frac{2}{L^2} \left(1 + \frac{1}{2}\Phi_a^2\right) + \mathcal{O}(\Phi_a^4) \approx -\frac{6}{L^2} - \sum_{a=1}^{3} \frac{1}{L^2}\Phi_a^2 \tag{2.1.23}$$

The constant term $-6/L^2$ generates the exact negative cosmological constant necessary to sustain the AdS_4 background, since in four dimensions $\Lambda = -3/L^2$.

By equating the quadratic terms in (2.1.23) to the standard classical definition of a scalar mass term, $\frac{1}{2}m_a^2\Phi_a^2$, we explicitly find that all three dilatons possess the exact same mass squared

$$m_1^2 = m_2^2 = m_3^2 = -\frac{2}{L^2}. \tag{2.1.24}$$

Comparing this to the BF bound, we see that $m_a^2 = -2/L^2 > -9/4L^2 = -2{,}25/L^2$. Therefore, all three scalar fields sit above the Breitenlohner-Freedman bound, confirming that the full supergravity vacuum is strictly stable against classical instabilities. This specific value is highly significant, as it corresponds to the conformal mass in four-dimensional AdS spacetime. As a consequence of this conformal symmetry, scalar perturbations around the global AdS background

effectively experience no potential [59].

Furthermore, substituting this mass into our expression for $\Delta_\pm$, (2.1.18), we get

$$\Delta_\pm = \frac{3}{2} \pm \sqrt{\frac{9}{4} - 2} = \frac{3}{2} \pm \frac{1}{2}. \tag{2.1.25}$$

This fixes the asymptotic behavior of the entire scalar sector of the STU model to

$$\Phi_a(r) \approx \frac{\alpha_a}{r} + \frac{\beta_a}{r^2} \quad \text{for } a = 1, 2, 3. \tag{2.1.26}$$

2.1.3. Asymptotic Analysis

To extract the holographic data from the solutions presented previously, we must analyze their behavior near the conformal boundary. In the coordinates of (2.1.9), the boundary is reached as the radial coordinate r goes to infinity. However, a direct expansion in r generally introduces $\mathcal{O}(1/r)$ fall-off terms across multiple metric components, which creates an ambiguity in the identification of the mass. Therefore, to bring the metric into a form that allows for a direct reading of the dual energy-momentum tensor, we must systematically eliminate these $\mathcal{O}(1/r)$ terms from the spatial and radial components, leaving them exclusively in g_{tt}, see [60]. To achieve this and simplify the comparison between different solutions, we introduce a new radial coordinate ρ defined by the following expansion

$$\begin{aligned} r =& \rho - \frac{1}{4}\sum_\Lambda q_\Lambda + \frac{1}{\rho}\left(\frac{3}{32}\sum_\Lambda q_\Lambda^2 - \frac{1}{16}\sum_{\Lambda_1<\Lambda_2} q_{\Lambda_1} q_{\Lambda_2}\right) \\ &- \frac{1}{32\rho^2}(q_1+q_2-q_3-q_4)(q_1-q_2+q_3-q_4)(q_1-q_2-q_3+q_4) + O(\rho^{-3}), \end{aligned} \tag{2.1.27}$$

where the indices labeled with Λ or Λ_i run from 1 to 4. This transformation ensures that the metric functions exhibit the appropriate fall-off conditions required for

asymptotically AdS_4 spaces

$$g_{xx} = g_{\varphi\varphi} = \frac{r^2}{L^2}\sqrt{H(r)} = \frac{\rho^2}{L^2} + O(\rho^{-2})\,, \tag{2.1.28}$$

$$-g_{tt} = \frac{f(r)}{\sqrt{H(r)}} = \frac{\rho^2}{L^2} - \frac{m}{\rho} + O(\rho^{-2})\,, \tag{2.1.29}$$

$$\begin{aligned} g_{\rho\rho} =& \frac{\sqrt{H(r)}}{f(r)}\left(\frac{dr}{d\rho}\right)^2 = \frac{L^2}{\rho^2} - \frac{L^2}{16\rho^4}\left(3\sum_{\Lambda} q_\Lambda^2 - 2\sum_{\Lambda_1<\Lambda_2} q_{\Lambda_1} q_{\Lambda_2}\right) \\ &+ \frac{L^2}{8\rho^5}\left(\sum_{\Lambda} q_\Lambda^3 - \sum_{\Lambda_1\neq\Lambda_2} q_{\Lambda_1}^2 q_{\Lambda_2} + 2\sum_{\Lambda_1<\Lambda_2<\Lambda_3} q_{\Lambda_1} q_{\Lambda_2} q_{\Lambda_3} + 8mL^2\right) + O(\rho^{-6})\,. \end{aligned} \tag{2.1.30}$$

Similarly, the scalar fields Φ_a must be expanded to identify their corresponding dual operators. As discussed in the section on the Breitenlohner-Freedman bound, a scalar field with $m^2L^2 = -2$ in AdS_4 admits the near-boundary behavior

$$\Phi_a(\rho) = \frac{\alpha_a}{\rho} + \frac{\beta_a}{\rho^2} + O(\rho^{-3})\,. \tag{2.1.31}$$

Both modes are normalizable, so one may choose either the standard or the alternative quantization. In the standard quantization, α_a is interpreted as the source and β_a as the VEV of an operator of dimension $\Delta = 2$. In the alternative quantization, the roles are exchanged, α_a is interpreted as the VEV of a dimension-one operator, while β_a is associated with the source. In this work, the STU solutions obey the alternative quantization with mixed boundary conditions. Therefore, the coefficients α_a will be interpreted as the scalar VEVs, while the coefficients β_a are fixed functions of them rather than independent sources. The asymptotic fall-off for the dilatons is given by

$$\Phi_1 = \frac{1}{2\rho}(q_1 + q_2 - q_3 - q_4) - \frac{1}{8\rho^2}(q_1 - q_2 - q_3 + q_4)(q_1 - q_2 + q_3 - q_4) + O(\rho^{-3})\,, \tag{2.1.32}$$

$$\Phi_2 = \frac{1}{2\rho}(q_1 - q_2 + q_3 - q_4) - \frac{1}{8\rho^2}(q_1 + q_2 - q_3 - q_4)(q_1 - q_2 - q_3 + q_4) + O(\rho^{-3})\,, \tag{2.1.33}$$

$$\Phi_3 = \frac{1}{2\rho}(q_1 - q_2 - q_3 + q_4) - \frac{1}{8\rho^2}(q_1 + q_2 - q_3 - q_4)(q_1 - q_2 + q_3 - q_4) + O(\rho^{-3})\,. \tag{2.1.34}$$

Comparing these expressions with the general expansion above, we identify the leading coefficients as

$$\alpha_1 = \frac{1}{2}(q_1 + q_2 - q_3 - q_4)\,, \tag{2.1.35}$$

$$\alpha_2 = \frac{1}{2}(q_1 - q_2 + q_3 - q_4)\,, \tag{2.1.36}$$

$$\alpha_3 = \frac{1}{2}(q_1 - q_2 - q_3 + q_4)\,. \tag{2.1.37}$$

The subleading coefficients are read from the $1/\rho^2$ terms. They are not independent, but satisfy

$$\beta_1 = -\frac{1}{2}\alpha_2\alpha_3\,, \qquad \beta_2 = -\frac{1}{2}\alpha_1\alpha_3\,, \qquad \beta_3 = -\frac{1}{2}\alpha_1\alpha_2\,. \tag{2.1.38}$$

This relation can be written compactly as a mixed boundary condition

$$\beta_i = -\frac{\partial W}{\partial \alpha_i}\,, \qquad W(\alpha) = \frac{1}{2}\alpha_1\alpha_2\alpha_3\,. \tag{2.1.39}$$

The function W its the function that encodes the mixed boundary conditions for the scalar sector. From the dual field theory point of view, it represents a triple-trace deformation. Since it is cubic in the dimension-one VEVs α_i, it has dimension three in the boundary CFT_3 and therefore preserves conformal invariance. Hence, these solutions possess conformally invariant boundary conditions relevant for the description of ABJM theory [61] (named after Aharony, Bergman, Jafferis, and Maldacena)[2]. This is the class of boundary conditions for which the holographic stress tensor and the mass can be consistently extracted by holographic renormalization [60].

For these boundary conditions the dual energy momentum tensor can be obtain following the procedure described in [60], yielding

$$\langle T_{\varphi\varphi}\rangle = \frac{m}{2\,\kappa\,L^2}\,, \qquad \langle T_{xx}\rangle = \frac{m}{2\,\kappa\,L^2}\,, \qquad \langle T_{tt}\rangle = \frac{m}{\kappa\,L^2}\,, \tag{2.1.40}$$

where we pick the following representative of the conformal boundary metric

$$ds^2_\partial = -dt^2 + dx^2 + d\varphi^2\,. \tag{2.1.41}$$

[2]Although defined on a $d = 3, \mathcal{N} = 6$ superspace for general levels, the specific sector dual to the STU model exhibits an enhancement to $\mathcal{N} = 8$ supersymmetry, providing a robust theoretical laboratory for solving complex problems in condensed matter physics.

This identification completes the mapping between the gravitational bulk parameters (m, q_Λ) and the thermodynamic variables of the dual field theory, providing the basis for the stability analysis that follows.

2.2. Black Hole Thermodynamics

The evolution in the study of black holes from being understood merely as solutions to General Relativity to complex thermodynamic systems is one of the most significant developments in modern physics. This evolution began in the early 1970's, when a series of conceptual puzzles started challenging this purely geometric view of these systems.

The first step toward this transition was the establishment of the no-hair theorems, developed in [62–65]. These proved that a stationary black hole is characterized solely by its mass M, angular momentum J, and charge Q. From a statistical perspective, this was paradoxical, it implied that a black hole has only a few degrees of freedom, despite being able to swallow an immense amount of matter with high entropy.

This led Jacob Bekenstein to question the consistency of the Second Law of Thermodynamics. If one could drop a high-entropy object into a black hole, say a cup of coffee, the total entropy of the visible universe would decrease, seemingly violating the law, see [66]. Bekenstein proposed that in order to save the Second Law, black holes must possess an intrinsic entropy proportional to the area of their event horizon A. His intuition was partially fueled by Stephen Hawking's 1971 discovery of the Area Theorem, in [67], which proved that $dA \geq 0$ in any classical process. Bekenstein suggested a new "Generalized Second Law", stating that the sum of the common entropy in the exterior and the black hole entropy must never decrease, see [68]. However, Bekenstein's proposal faced serious doubts from the physics community. If a black hole had entropy, it necessarily implied it had a non-zero temperature, and according to the Stefan-Boltzmann law, any object with temperature must radiate. Classically, this was impossible, as nothing was thought to be able to escape the gravitational pull of a black hole.

The conceptual disaster was broken in 1975 when Stephen Hawking applied the framework of quantum field theory to a curved background. He demonstrated that vacuum fluctuations near the event horizon lead to the creation of particle-

antiparticle pairs, where one member falls into the hole while the other escapes to infinity, [69]. This process, known as Hawking radiation, proved that black holes emit a thermal spectrum of particles with a temperature proportional to their surface gravity κ

$$T = \frac{\kappa}{2\pi}. \tag{2.2.1}$$

This discovery provided the missing physical link to Bekenstein's work. By identifying the physical temperature, the constant of proportionality for the entropy was fixed, leading to the celebrated Bekenstein-Hawking formula

$$S = \frac{A}{4G}. \tag{2.2.2}$$

Following these breakthroughs, the analogies between gravitation and thermodynamics were systematized into the Four Laws of Black Hole Mechanics [70].

This systematization started a new branch of theoretical physics dedicated to the study of the thermodynamics of gravitational objects, abandoning the purely geometrical description of these objects.

Furthermore, the significance of these thermodynamic properties acquired a new and profound brilliance with the advent of the AdS/CFT correspondence [1]. Within this holographic framework, an asymptotically Anti-de Sitter black hole is no longer viewed only as an isolated gravitational entity, but as the dual representation of a thermal state in a strongly coupled conformal field theory (CFT) residing on the conformal boundary.

In this context, the thermodynamic variables of the black hole, such as its temperature T, entropy S, and chemical potentials μ, map directly to the physical properties of a dual thermal plasma. This correspondence allows us to interpret the stability and phase transitions of the gravitational bulk as the equilibrium conditions and phase structure of the dual quantum system. The study of the thermodynamics and holographic description of the classical black hole solutions has been studied in detail in many works, for example, see [7, 71, 72]. In this context, the study of the STU black hole configurations presented in this work

provides a rigorous method for investigating complex thermal phenomena, such as the confinement-deconfinement transition, in the non-perturbative regime of holographic field theories.

For the purposes of this thesis, the STU model provides a naturally rich landscape for exploring these thermodynamic properties. Furthermore, because the STU model is a consistent truncation that can be uplifted to the maximal gauged $\mathcal{N} = 8$ supergravity and ultimately to M-theory, it serves as a powerful holographic bridge. This connection enables the description of strongly coupled thermal plasmas in the dual field theory, such as the ABJM theory, that would otherwise be inaccessible through standard perturbative methods, offering a unique window into the non-perturbative regime of quantum field theory.

2.2.1. Stability: Global vs Local

In classical thermodynamics, the very definition of an equilibrium state is intrinsically connected to the concept of stability. For a macroscopic system to possess well-defined thermodynamic coordinates, such as temperature, entropy, or chemical potential, it must be resilient against fluctuations. Stability ensures that when a system experiences a deviation from its equilibrium configuration, natural interaction forces of the system drive it back to its initial state. Without this property, the notion of a persistent, measurable thermodynamic state collapses.

To rigorously classify equilibrium, we must distinguish between two fundamentally different types of stability, local and global.

Local stability pertains to the response of a system to infinitesimal perturbations around an equilibrium state. To ilustrate this, consider a thermodynamic system characterized by its internal energy E, which is a function of a set of extensive variables $x^a = (S, Q_1, Q_2, \ldots, Q_n)$, where S is the entropy and Q_i represent other conserved charges such as volume, particle number, or in the case of black holes, electric and magnetic charges. The first derivatives of the fundamental relation define the intensive variables conjugate to the extensive coordinates. Thus

$$y_a = \frac{\partial E}{\partial x^a}, \qquad T = \frac{\partial E}{\partial S}, \qquad \mu_i = \frac{\partial E}{\partial Q_i}. \tag{2.2.3}$$

In the microcanonical ensemble, the fundamental criterion for equilibrium is the

maximum entropy principle. An isolated system reaches equilibrium when its total entropy is maximized among all accessible states with fixed total energy and fixed conserved charges. Equivalently, one may use the dual energy principle, in which the total energy is minimized at fixed total entropy and fixed conserved charges. This equivalent formulation is useful because the thermodynamic information is encoded in the energy representation $E(x^a)$. In gravitational thermodynamics, the accessible macroscopic states are represented by classical geometries solving the equations of motion. These geometries are the saddles of the gravitational path integral, for example black holes, thermal AdS backgrounds, or solitons. Each saddle carries its own thermodynamic relation $E(x^a)$ and must first be tested for local stability before it can be compared globally with other saddles.

To see how the stability criterion arises, imagine an isolated system divided into two neighbouring subsystems A and B. The total extensive quantities are fixed, while the two parts may exchange entropy and charge through internal fluctuations. If x^a_A denotes the extensive coordinates of subsystem A, conservation implies

$$\delta x^a_A + \delta x^a_B = 0, \qquad \delta x^a_B = -\delta x^a_A. \tag{2.2.4}$$

The total energy is

$$E_{\text{tot}} = E_A(x^a_A) + E_B(x^a_B). \tag{2.2.5}$$

Expanding around an equilibrium configuration gives

$$\delta E_{\text{tot}} = \sum_a \left(\frac{\partial E_A}{\partial x^a_A} - \frac{\partial E_B}{\partial x^a_B} \right) \delta x^a_A + \frac{1}{2} \sum_{a,b} \left(\frac{\partial^2 E_A}{\partial x^a_A \partial x^b_A} + \frac{\partial^2 E_B}{\partial x^a_B \partial x^b_B} \right) \delta x^a_A \delta x^b_A + \mathcal{O}(\delta x^3). \tag{2.2.6}$$

The first-order term gives the equilibrium conditions. Since $\partial E/\partial x^a$ are the intensive variables, its vanishing requires equality of the intensive parameters between the two subsystems. In particular

$$T_A = T_B, \qquad \mu^A_i = \mu^B_i. \tag{2.2.7}$$

Thus the linear term vanishes because the system is expanded around an equilibrium configuration. Once this condition is imposed, local stability is determined by the second variation. The energy minimum principle requires

$$\delta^{(2)} E_{\text{tot}} = \frac{1}{2} \sum_{a,b} \left(H^A_{ab} + H^B_{ab} \right) \delta x^a_A \delta x^b_A > 0 \tag{2.2.8}$$

for every non-trivial allowed redistribution of the extensive variables, where H^A_{ab} and H^B_{ab} denote the Hessians of the two subsystems. This expression shows that stability is a statement about the response of the saddle under study together with the response of the environment with which it exchanges conserved quantities.

The passage to a criterion for a single gravitational solution is obtained by considering the environment as a stable reservoir. The role of the reservoir is to enforce the equilibrium values of the intensive variables and to absorb the compensating fluctuation required by the conservation laws. In the reservoir limit, the environment is assumed to be thermodynamically stable and sufficiently large that its intensive variables remain fixed under the compensating fluctuation. A negative direction in the Hessian of the saddle under study then gives an allowed fluctuation that lowers the total energy and signals a genuine local instability. Equivalently, one may divide a homogeneous phase into two identical neighbouring subsystems. In that case $H^A_{ab} = H^B_{ab} = H_{ab}$, so the second variation contains $H^A + H^B = 2H$. Positivity of $H^A + H^B$ is therefore exactly equivalent to positivity of the Hessian of either subsystem. Therefore local stability can be tested intrinsically from the fundamental relation of a single saddle. Writing the perturbation simply as δx^a, the relevant second-order variation is

$$\delta E = \frac{1}{2} \sum_{a,b} \frac{\partial^2 E}{\partial x^a \partial x^b} \delta x^a \delta x^b + \mathcal{O}(\delta x^3). \tag{2.2.9}$$

From (2.2.9) we see that for the state to be stable against fluctuations, the energy must increase under every allowed internal redistribution. Therefore, in the energy representation, local stability requires the quadratic form to be strictly positive. This implies that the Hessian matrix of the energy, defined as

$$\mathcal{H}_{ab} = \frac{\partial^2 E}{\partial x^a \partial x^b}, \tag{2.2.10}$$

must be positive definite. Physically, the elements of this Hessian matrix encode the so-called response functions of the system. For instance, the condition $\partial^2 E/\partial S^2 > 0$ is equivalent to requiring a positive specific heat, $C_Q = T(\partial S/\partial T)_Q > 0$ at fixed charge. If the Hessian ceases to be positive definite, meaning it develops a negative eigenvalue, the system reaches a spinodal point and becomes locally unstable. A locally unstable state cannot be physically realized as a steady state, as any infinitesimal perturbation will cause it to rapidly evolve away from that configuration. Once each gravitational saddle has passed this local test, global stability is decided separately by comparing the corresponding thermodynamic potentials. This is the step in which one compares black holes against other classical backgrounds such as thermal AdS or AdS solitons.

Global stability, on the other hand, evaluates the competition between distinct, globally separated macroscopic states. A configuration might be a local minimum of the energy or free energy (thus being locally stable, or metastable), but not the absolute lowest energy state available to the system.

To understand mathematically why the configuration with the minimum free energy is the "privileged" one, we must shift our perspective to statistical mechanics and consider ensembles where the energy is no longer fixed, but considered a random variable. In the canonical ensemble, a system is in thermal contact with a heat bath at a fixed temperature $T = 1/\beta$. Because the system continuously exchanges heat with the reservoir, its internal energy fluctuates. The probability P_i of finding the system in a specific microstate i with energy E_i is given by the Boltzmann distribution, given by

$$P_i = \frac{1}{Z} e^{-\beta E_i}, \tag{2.2.11}$$

where $Z = \sum_i e^{-\beta E_i}$ is the partition function. The bridge to thermodynamics is established through the Helmholtz free energy, $F = -\beta^{-1} \ln Z$. Now, suppose our system can exist in two distinct macroscopic phases, A and B, each containing a vast number of microstates. The probability of finding the system in phase A versus phase B is proportional to the sum of the Boltzmann weights of their respective microstates, which can be written entirely in terms of their macroscopic free energies, F_A and F_B

$$\frac{P_A}{P_B} = \frac{e^{-\beta F_A}}{e^{-\beta F_B}} = e^{-\beta(F_A - F_B)}. \tag{2.2.12}$$

In the thermodynamic limit (where the number of degrees of freedom $N \to \infty$), the free energy scales extensively with the size of the system. Therefore, even a microscopically small difference in the free energy leads to an exponentially large difference in the relative probabilities of the two phases. If $F_A < F_B$, the ratio $P_A/P_B \to \infty \Rightarrow P_B/P_A \to 0$. The probability of the system occupying phase B becomes exponentially suppressed, proving that the state with the lowest free energy is the overwhelmingly probable, and thus a globally stable configuration.

In the context of black hole thermodynamics, these classical concepts map onto the geometric properties of spacetime, leading to the study of the thermodynamic stability of black holes. A classic example that would be the first thing one would analyze, is the Schwarzschild black hole in asymptotically flat space, one can show that this black hole possesses a negative specific heat ($\mathcal{H}_{SS} < 0$) and is thus inherently thermodynamically locally unstable, which makes the study of this solution seem a bit uninteresting at first sight. However, the thermodynamic landscape transforms dramatically when we modify the asymptotic structure of spacetime. In asymptotically Anti-de Sitter (AdS) spacetimes, the negative cosmological constant effectively acts as a reflecting boundary, or a confining box for the system. This confinement stabilizes the thermodynamics, allowing for the existence of locally stable configurations, such as large Schwarzschild-AdS black holes that possess a positive specific heat.

The richness of the phase space increases significantly when we introduce additional conserved charges, such as the electric charge Q in the Reissner-Nordström-AdS solution. The extensive variables now form a vector $x^a = (S, Q)$, and the corresponding intensive parameters are the temperature T and the electric potential Φ. Consequently, the Hessian matrix $\mathcal{H}_{ab}$ becomes a 2×2 matrix. For this charged black hole to be locally stable, the entire Hessian must be positive definite. This requires not only a positive specific heat at constant charge ($C_Q > 0$), but also a positive adiabatic electrical capacitance (or susceptibility), encoded in the requirement that $\partial^2 E/\partial Q^2 = (\partial\Phi/\partial Q)_S > 0$, alongside a positive determinant for the full matrix.

However, there are cases where the richness of black hole phase spaces emerges

precisely from the regions where local stability ceases to exist. Within these so-called spinodal regions, the instability often gives way to an alternative, and sometimes previously unknown, stable phase. This phenomenon is a central theme in this work. In this context, we analyze the phase space of planar black holes, relying on the Hessian of the energy, $\mathcal{H}_{ab}$, to strictly map their stability bounds. There exist regions in the parameter space where the eigenvalues of the Hessian change sign, meaning these planar black holes reach a spinodal point and lose their local stability.

Naively, one might expect this local instability to simply truncate the physical phase space, leaving an otherwise featureless or boring diagram where black holes simply cease to exist. However, we demonstrate that this region is not merely empty, it is physically "filled" by a radically different class of solutions, AdS solitons. We show that the loss of local stability for planar black holes precisely paves the way into these horizonless solitonic geometries.

2.2.1.1. Sylvester Criterion

To rigorously establish the local thermodynamic stability of the system, we must ensure that the Hessian matrix of the mass is strictly positive definite. While evaluating the exact eigenvalues is the most direct approach to verify matrix definiteness, the characteristic polynomial for a multidimensional thermodynamic parameter space can often be analytically intractable. In such scenarios, the Sylvester criterion provides a powerful and equivalent algebraic method to determine stability. The Sylvester criterion states that a real symmetric matrix is positive definite if and only if all of its leading principal minors are strictly positive. A leading principal minor M_k of order k is defined as the determinant of the upper left $k \times k$ submatrix. For our specific system, the extensive variables define a five dimensional parameter space, meaning the Hessian $\mathcal{H}_{\lambda\sigma}$ is a 5×5 symmetric matrix. Therefore, the criterion dictates that local stability is mathematically guaranteed if and only if the entire sequence of five leading principal minors is strictly positive

$$M_1 > 0, \quad M_2 > 0, \quad M_3 > 0, \quad M_4 > 0, \quad M_5 = \det \mathcal{H} > 0. \tag{2.2.13}$$

During the evaluation of our planar black hole solution, computing the lower order

principal minors (M_1 through M_4) reveals that they are either manifestly positive for parameters or they impose broad constraints that are naturally satisfied within the physical domain. The critical and most restrictive boundaries of the stability region are fundamentally governed by the final principal minor, which is the full determinant of the Hessian matrix.

Consequently, when the black hole approaches a thermodynamic instability, it is the full determinant M_5 that first vanishes, signaling that at least one eigenvalue has crossed zero to become negative. This mathematical property formally justifies our analytical methodology.

2.2.2. Analyticity and Phase Transitions

It is very common in a thermodynamic context to use the terms "phase" and "transition" vaguely, without being clear about what these concepts represent. While intuitively familiar from everyday experience, they hide profound mathematical subtleties that require careful analysis for our proper understanding, especially in the context of black hole thermodynamics.

Mathematically, a phase is strictly defined as an open, continuous region in the parameter space of intensive variables (such as temperature T and chemical potentials μ_i) where the thermodynamic potential, and consequently all its derivatives, is a single-valued, smooth, and entirely analytical function. Physically, this means the system exists in a stable, well-defined macroscopic configuration with a specific internal organization. This means that, as long as we smoothly vary the control parameters within this analytical domain, the macroscopic properties of the system respond smoothly and predictably.

A phase transition is the boundary between these regions. It is the precise locus in the parameter space where the analyticity of the free energy breaks down. But how does an analytical function suddenly become non-analytical?

For a system with a finite number of degrees of freedom, Z is a finite sum of positive exponential terms. The logarithm of a finite sum of positive analytical functions is always analytical. Therefore, strictly speaking, a finite system cannot undergo a phase transition. The non-analytical behavior required for a phase transition can only emerge in the thermodynamic limit, where the number of degrees of freedom approaches infinity ($N \to \infty$). In this limit, the sum becomes

an integral, and the roots of the partition function can pinch the real axis of the physical parameters, manifesting as singularities or discontinuities in the free energy.

When we say a system "transitions", it means that as we tune an external parameter such as the temperature, the global minimum of the free energy shifts abruptly from one analytical branch to another. The system is physically forced to globally reorganize its degrees of freedom to adopt the new configuration that minimizes the thermodynamic potential.

The Ehrenfest Classification:

Historically, Paul Ehrenfest classified these breaks in analyticity based on the lowest-order derivative of the free energy that exhibits a discontinuity at the critical transition point.

- First-Order Phase Transitions: These occur when the first-order derivatives of the thermodynamic potential are discontinuous. For instance, the entropy S and the conserved charges Q_i are defined as the first derivatives of the free energy with respect to temperature and chemical potentials, respectively. A phase transition is of first order if the branches of the free energy for two distinct phases cross at a sharp angle. At the coexistence line, the system jumps from one branch to the other, causing a discrete jump in S and Q_i. Physically, the discontinuity in entropy manifests as latent heat ($L = T_c \Delta S$), meaning the system must absorb or release finite energy to completely reconstruct its macroscopic state from one phase to the other.
- Second-Order (and Higher-Order) Phase Transitions: In these transitions, the free energy branches meet tangentially. The first derivatives remain perfectly continuous (thus, there is no latent heat or jump in charge), but the second-order derivatives are discontinuous or divergent. The response functions, which constitute the Hessian matrix discussed in the previous section, such as the specific heat C_Q or the generalized susceptibilities χ_{ij}, carry this information.

When extending these classical concepts to gravity, particularly in asymptotically Anti-de Sitter (AdS) spacetimes, we face a conceptual challenge: what plays the role of the thermodynamic limit, and how do we define the free energy of an

infinite spacetime?

Through the AdS/CFT correspondence, the thermodynamic limit ($N \to \infty$ in the dual boundary conformal field theory) elegantly translates to the semi-classical limit of the bulk gravitational theory ($G_N \to 0$), for a pedagogical description of this feature of the holographic dictionary, see [73]. In this regime, the gravitational path integral is extremely dominated by its classical saddle points, the classical solutions to the equations of motion. Thus, competing thermodynamic phases in gravity simply correspond to different classical geometries (saddle points) that share the same asymptotic boundary conditions.

To extract the thermodynamic variables without ambiguities, we rely on holographic renormalization. The macroscopic state variables, such as the total mass (energy) M of the spacetime, can be rigorously extracted by computing the holographic stress-energy tensor $T_{\mu\nu}$ defined at the asymptotic boundary. Once M, the entropy S, and the physical charges Q_i are identified, we can construct the appropriate free energy for our ensemble, for instance, the grand potential $G = M - TS - \sum \mu_i Q_i$.

The study of these transitions in a gravitational theory shows us that different geometric structures can decay or transition into others. In the rich parameter space of models like gauged $\mathcal{N} = 8$ supergravity, the landscape is vast, since this theory has multiple chemical potentials and charges. The condition for a phase transition between two competing geometries, such as a planar black hole and an AdS soliton (as it will be our case), is the equality of their free energies

$$G_{\mathrm{BH}}(T, \mu_i) = G_{\mathrm{soliton}}(T, \mu_i), \tag{2.2.14}$$

At this coexistence line, the thermodynamic system inherently chooses the geometry with the lowest free energy. Because the planar black hole and the AdS soliton are topologically and geometrically distinct, the first possessing an event horizon, and thus, finite entropy, and the other being a horizonless smooth geometry, thus having zero entropy. Therefore, the transition between them is strictly first-order, characterized by a discrete jump in one of the first derivatives of the free energy, the entropy.

This formal framework is exactly what allows us to “fill” the spinodal regions

where the planar black hole loses its local stability. By computing the holographic free energy of both configurations, we can rigorously demonstrate that it is always possible to complete the phase space with AdS solitons by undergoing a first-order phase transition into the solitonic phase, yielding a rich thermodynamic phase space.

2.2.3. Hawking Page and Confinement

To fully understand the physical implications of phase transitions in Anti-de Sitter (AdS) spacetimes, we must look at them through the lens of the AdS/CFT correspondence.

A typical, and the original example of the AdS/CFT correspondence is the duality between Type IIB string theory on $AdS_5 \times S^5$ and $\mathcal{N} = 4$ Super Yang-Mills theory. This boundary theory is a gauge theory with an $SU(N)$ gauge group, conceptually similar to Quantum Chromodynamics (QCD) but with additional supersymmetries. Here, N represents the rank of the gauge group, often referred to as the number of "colors". The fundamental degrees of freedom of this theory, such as gluons, transform in the adjoint representation of $SU(N)$. This means the total number of interacting degrees of freedom in a deconfined plasma scales as N^2 for large N. On the contrary, in a confined phase, these gluons group together into color singlet states (like hadrons), and the number of degrees of freedom drops significantly to a quantity of order $\mathcal{O}(1)$.

We can map these phases to gravity by looking at the entropy. According to the holographic dictionary, the inverse of Newton's constant $1/G_N$ is proportional to N^2. Since a black hole has an event horizon, its classical Bekenstein-Hawking entropy is proportional to the horizon area divided by G_N. Therefore, the entropy of any black hole scales exactly as N^2. This provides a clear physical conclusion: *a black hole in AdS is the holographic dual of the deconfined plasma phase.*

Now we must ask what the gravitational dual of the confined phase is. To find it, we need a bulk geometry that satisfies the exact same boundary conditions at infinity as the black hole. Specifically, it must have the same temperature T at the AdS boundary, but it cannot have an event horizon. This reference geometry is known as Thermal AdS. It is simply the empty AdS spacetime filled with a thermal gas of non-interacting particles. Because Thermal AdS has no horizon,

its classical Bekenstein-Hawking entropy is exactly zero. The only entropy comes from the quantum thermal gas itself, which does not scale with N^2. Its entropy is strictly of order $\mathcal{O}(1)$, *making Thermal AdS the perfect holographic dual for the confined phase.*

With this dictionary in place, we can study the Schwarzschild-AdS black hole with spherical horizon in four dimensions. The full line element for this solution is given by

$$ds^2 = -f(r)dt^2 + \frac{dr^2}{f(r)} + r^2 d\Omega_2^2 \tag{2.2.15}$$

where $d\Omega_2^2$ is the metric of the unit two-sphere, and the metric function is

$$f(r) = 1 - \frac{2m}{r} + \frac{r^2}{L^2}, \tag{2.2.16}$$

Here m is related to the ADM mass of the black hole, M, suitably generalized to asymptotically AdS geometries [74], and L is the AdS radius. The event horizon is located at the largest positive root of the metric function, $f(r_h) = 0$. The black hole mass is given by

$$M = \frac{2\sigma}{\kappa} m. \tag{2.2.17}$$

Here $\kappa = 8\pi G$, and σ denotes the volume of the unit two-sphere, $\sigma = 4\pi$. From the horizon condition, the mass parameter can be written in terms of the horizon radius as $m = r_h(1 + r_h^2/L^2)/2$. Thus,

$$M = \frac{\sigma}{\kappa} r_h \left(1 + \frac{r_h^2}{L^2}\right). \tag{2.2.18}$$

The Hawking temperature is given by the surface gravity evaluated at the horizon, $T = f'(r_h)/(4\pi)$, which results in

$$T = \frac{1 + 3r_h^2/L^2}{4\pi r_h}. \tag{2.2.19}$$

If we solve for the horizon radius r_h, we find two configurations compatible with

the same temperature. These are called the small black hole and the large black hole, with radii given by

$$r_h^{(\pm)} = \frac{L}{3}(2\pi LT \pm \sqrt{4\pi^2 L^2 T^2 - 3}). \tag{2.2.20}$$

From (2.2.20) we see that for a horizon to exist, the inequality $4\pi^2 L^2 T^2 - 3 \geq 0$ must hold. This implies that these black hole configurations have a minimum temperature, given by

$$T_{\text{min}} = \frac{\sqrt{3}}{2\pi L}. \tag{2.2.21}$$

It is useful to introduce the dimensionless horizon radius $\xi := r_h/L$. Also, we introduce a dimensionless temperature, $\tau := LT$, such that the minimum temperature is given by $\tau_{\text{min}} = \sqrt{3}/2\pi$. Given these new dimensionless quantities, we see they are related by (2.2.20) as

$$\xi^{(\pm)} = \frac{1}{3}\left(2\pi\tau \pm \sqrt{4\pi^2\tau^2 - 3}\right). \tag{2.2.22}$$

The behavior of the two horizon-radius branches compatible with the same temperature is shown in figure 2.2.1.

Finally, the entropy is determined by the Bekenstein-Hawking area law (2.2.2), which we can rewrite as

$$S = \frac{A}{4G} = \frac{2\pi A}{\kappa} = \frac{2\pi\sigma}{\kappa} r_h^2, \tag{2.2.23}$$

where we have used $A = \sigma r_h^2$, recall $\sigma = 4\pi$.

For a given boundary temperature T, both Thermal AdS and the spherical black hole are valid classical solutions. To determine which one the system prefers, we compute their free energies. Taking Thermal AdS as our reference state with $F_0 = 0$, the free energy of the black hole is computed directly from our thermodynamic quantities (2.2.18), (2.2.19) and (2.2.23), substituting in $F = M - TS$, we get

$$F(r_h) = \frac{\sigma}{2\kappa} r_h \left(1 - \frac{r_h^2}{L^2}\right). \tag{2.2.24}$$

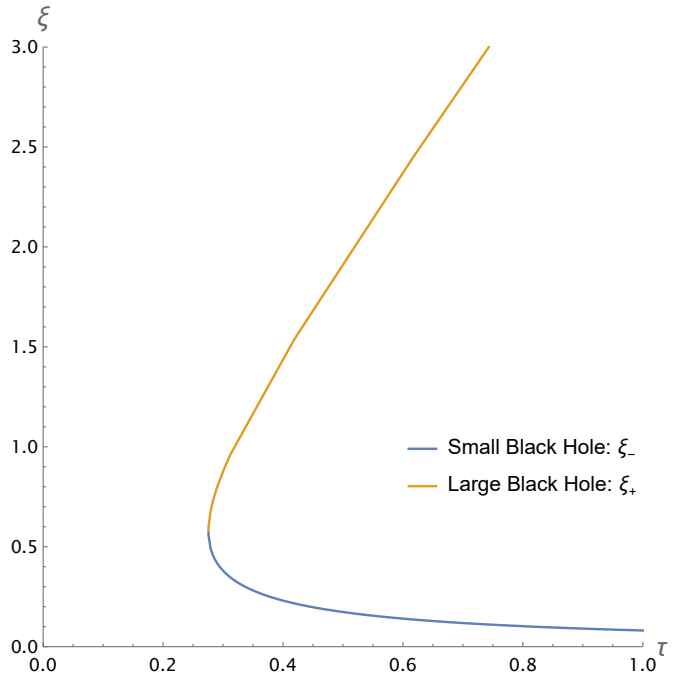

Figura 2.2.1: Dimensionless temperature τ versus the two dimensionless horizon-radius branches $\xi^{(\pm)}$ of the four-dimensional Schwarzschild-AdS black hole. The orange curve represents the large black hole, while the blue curve represents the small black hole.

This can be written in terms of the dimensionless horizon radius as

$$F(\xi) = \frac{L\sigma}{2\kappa}\xi\left(1-\xi^2\right). \tag{2.2.25}$$

Notice that if the black hole horizon fulfills the condition $\xi < 1$, its free energy is positive, $F > 0$. This means the confined phase (Thermal AdS) has a lower energy and is more stable. However, as one can see from (2.2.19), the large black hole increases as the temperature increases. When $\xi > 1$, the free energy becomes negative, $F < 0$, and the black hole becomes the globally stable state. This crossing point at $F = 0$ is the Hawking-Page transition, which represents the holographic confinement to deconfinement phase transition. Furthermore, in this case it is possible to locate the critical temperature at which this transition takes place, by imposing $F(\xi) = 0$. Since this gives $\xi = 1$, the transition must be evaluated on the $\xi^{(+)}$ branch, corresponding to the large black hole. Replacing this value in (2.2.22), we find the so-called Hawking-Page temperature, given by the dimensionless temperature

$$\tau_{\mathrm{HP}} = \frac{1}{\pi}. \tag{2.2.26}$$

It is worth emphasizing that the small black hole branch has negative heat capacity, making it a locally unstable branch (thus, not a thermal state in equilibrium, as we explained in the previous section), while the large black hole branch has positive heat capacity, making it a locally stable branch and the globally stable phase above the Hawking-Page temperature.

Having computed the free energy $F(\xi)$ for the Schwarzschild-AdS black hole in four dimensions, it is worth pausing to reflect on what quantity is most natural to analyze in the context of the AdS/CFT correspondence. As we have said, the black hole in four dimensions is dual to a thermal state of a Conformal Field Theory living on the three-dimensional conformal boundary. A defining feature of a CFT is the absence of any intrinsic mass scale, which means that temperature T is the sole energy scale available in the thermal ensemble. As a direct consequence of this conformal symmetry one finds that the free energy must scale as $F \sim T^3$. This is a requirement of conformal invariance. This way, dividing the free energy by T^3 removes the only dimensionful scale in the problem and yields a quantity whose non-trivial content reflects purely the structure of the phase space.

Now, the natural question is how to render this quantity fully dimensionless so that it can be meaningfully plotted and compared across different regimes. Starting from (2.2.25), one observes that F carries dimensions $[F] = [L]/[\kappa] = [L]^{-1}$, consistent with an energy. Now dividing by T^3 yields

$$\frac{F}{T^3} = \frac{L^3 F}{\tau^3} = \frac{L^4 \sigma}{2\kappa} \frac{\xi(1-\xi^2)}{\tau^3}, \tag{2.2.27}$$

Note that in this case we are working with the total free energy F rather than a free energy density. Since the boundary theory lives on the two-sphere S^2 of radius L with area $\mathrm{Vol}(S^2) = \sigma L^2$, the properly normalized free energy density is

$$\mathcal{F} = \frac{F}{\sigma L^2}. \tag{2.2.28}$$

Thus, we can consider

$$\frac{\mathcal{F}}{T^3} = \left(\frac{L^2}{\kappa}\right) \frac{\xi(1-\xi^2)}{2\tau^3}. \tag{2.2.29}$$

The factor L^2/κ is dimensionless in four dimensions, since $[\kappa] = [L]^2$, and $\mathcal{F}/T^3$ is already dimensionless by itself. Nevertheless, factoring out L^2/κ explicitly is physically meaningful. Through the AdS/CFT dictionary, this combination is directly proportional to the effective number of degrees of freedom of the dual theory. For the ABJM theory dual to AdS_4, one has $L^2/\kappa \propto k^{1/2}N^{3/2}$, where N is the rank of the gauge group and k is the Chern-Simons level. It is therefore natural to define the dimensionless free energy density by factoring out precisely this prefactor,

$$\widetilde{F} := \left(\frac{\kappa}{L^2}\right) \frac{\mathcal{F}}{T^3} = \frac{\xi(1-\xi^2)}{2\tau^3}, \tag{2.2.30}$$

which is independent of σ, κ, L and N. Figure 2.2.2 shows this dimensionless free energy. This is not the standard Hawking-Page plot of the un-normalized free energy, where the large black hole branch rapidly goes to $-\infty$ at high temperature. That behavior mainly reflects the CFT scaling $F \sim -T^3$. By dividing by T^3, we remove this leading temperature dependence and make the important information easier to see. Notice that the Hawking-Page transition still takes place at $\widetilde{F} = 0$, since the normalization by T^3 does not change the sign of the free energy. It also does not modify the minimum temperature, which is fixed by the existence of the black hole branches. Thus, the dimensionless plot keeps the relevant physical information intact while providing a clearer holographic description.

The Planar Limit and the AdS Soliton:

An important issue arises when we study the planar topology, which is the main focus of our work in the STU model.

We can mathematically derive the planar black hole by zooming into a small patch of the spherical horizon. We introduce a dimensionless scaling parameter λ and perform the following coordinate transformations to the metric (2.2.15)

$$r \to \lambda r, \quad t \to \frac{t}{\lambda}, \quad m \to \mu\lambda^3. \tag{2.2.31}$$

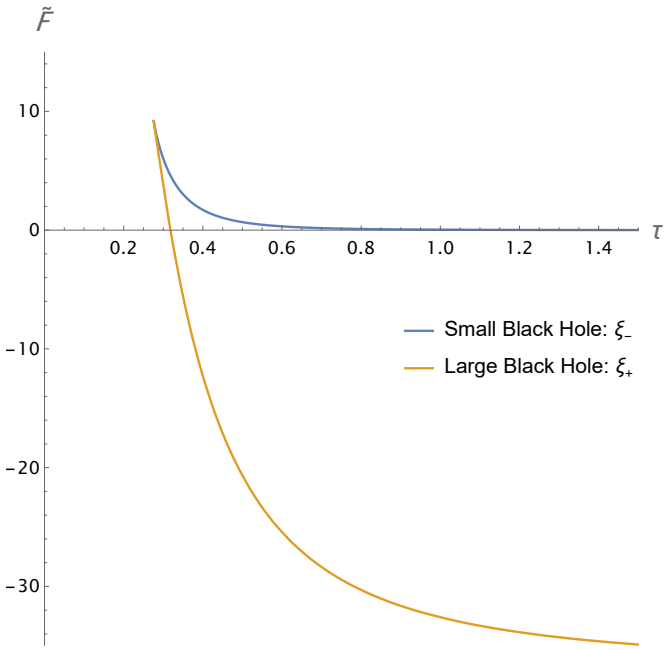

Figura 2.2.2: Dimensionless free energy density $\widetilde{F}$ versus dimensionless temperature τ for the two black hole branches. Dividing by T^3 removes the leading high-temperature scaling and highlights the Hawking-Page crossing. In orange the large black hole, in blue the small black hole.

Simultaneously, we flatten the solid angle $d\Omega_2^2$ into Cartesian coordinates $d\vec{x}^2$ by scaling the transverse space as $\vec{x} \to \vec{x}/\lambda$. Substituting these rescalings into the spherical metric function, we obtain

$$f(\lambda r) = 1 - \frac{2\mu\lambda^3}{\lambda r} + \frac{\lambda^2 r^2}{L^2} = \lambda^2 \left(\frac{1}{\lambda^2} - \frac{2\mu}{r} + \frac{r^2}{L^2} \right). \tag{2.2.32}$$

By substituting $f(\lambda r)$ into the scaled line element and taking the limit $\lambda \to \infty$, the constant term $1/\lambda^2$ vanishes completely. The line element reduces exactly to the planar topology

$$ds^2_{\text{planar}} = -\left(\frac{r^2}{L^2} - \frac{2\mu}{r} \right) dt^2 + \frac{dr^2}{\left(\frac{r^2}{L^2} - \frac{2\mu}{r} \right)} + r^2 d\vec{x}^2, \tag{2.2.33}$$

where the transverse part of the metric can be written in the form $d\vec{x}^2 = dx^2 + dy^2$. Notice that the constant 1 in the metric function $f(r)$ has disappeared, implying that the transverse sections of any fixed-r hypersurface are intrinsically flat.

At this point, regarding the thermodynamics, a fundamental distinction must

be made. Unlike the spherical black hole, the transverse space $\mathbb{R}^2$ of the planar geometry has infinite volume. Consequently, the total mass, entropy, and free energy are formally infinite. To formulate a meaningful thermodynamic framework, we factor out this transverse area and work with thermodynamic densities. Hence, for planar topologies, quantities such as $M = \epsilon$, s, and $\mathcal{F}$ denote the mass density (energy density), entropy density, and free energy density, respectively.

Also, in this case there is only one horizon radius for every positive temperature. Indeed, $T_{\text{planar}} = 3r_h/(4\pi L^2)$, or equivalently $\tau_{\text{planar}} = LT_{\text{planar}} = 3\xi/(4\pi)$. Recalculating the free energy density $\mathcal{F}$ for this planar black hole yields

$$\mathcal{F}_{\text{planar}} = -\frac{1}{2\kappa}\frac{r_h^3}{L^4} = -\frac{32\pi^3}{27}\frac{L^2}{\kappa}T_{\text{planar}}^3. \tag{2.2.34}$$

which is strictly negative for any temperature $T_{\text{planar}} > 0$. The consequence is clear, the planar black hole always dominates over the planar thermal gas. Moreover, following the same logic as in the spherical case, the dimensionless combination obtained after dividing by the natural CFT scaling is

$$\frac{\mathcal{F}}{T_{\text{planar}}^3} = -\left(\frac{L^2}{\kappa}\right)\frac{32\pi^3}{27}, \tag{2.2.35}$$

this is a constant negative value for all temperatures. Thus, the crossing of free energies never occurs, meaning there is no Hawking-Page transition. Let's recall, as it was explained in the planar case the factor L^2/κ carrys important information about the dual gauge theory, but we shall factor it out in order to define a quantity independent of the system of units

$$\widetilde{\mathcal{F}}_{\text{planar}} = \left(\frac{\kappa}{L^2}\right)\frac{\mathcal{F}}{T_{\text{planar}}^3} = -\frac{32\pi^3}{27}. \tag{2.2.36}$$

See figure 2.2.3. The dual field theory on a flat boundary remains permanently deconfined.

To restore a confined phase in the planar case, we need a different background geometry. If we compactify one of the spatial boundary coordinates on a circle, we can construct the AdS soliton, famously introduced by Horowitz and Myers in [33]. Obtained via a double Wick rotation of the planar black hole, as we saw

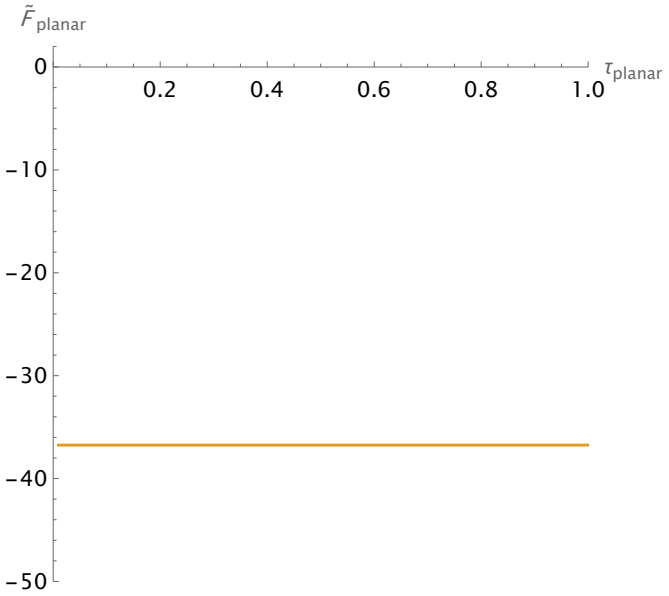

Figura 2.2.3: Normalized free energy density $\widetilde{F}_{\text{planar}}$ versus dimensionless temperature τ_{planar} for the planar Schwarzschild-AdS black hole. Since $\widetilde{F}_{\text{planar}}$ is constant and negative, there is no Hawking-Page transition with respect to the planar thermal gas.

in 2.1.1, the AdS soliton is a smooth geometry that possesses no horizon, merely capping off at a finite radial distance.

Crucially, because it lacks a horizon, its classical entropy is strictly zero, making it an $\mathcal{O}(1)$ state. This makes the AdS soliton the true holographic candidate for the confined vacuum. The thermodynamic competition in planar topologies is therefore not between a black hole and a thermal gas, but between a planar black hole and an AdS soliton.

Let's look at this closely. One way to obtain the AdS soliton solution is to consider the planar Schwazschild-AdS solution (2.2.33), where we must compactify one of the transverse coordinates, we will consider $\vec{x} = (x, y) = (\varphi, y)$, being φ identified with some arbitrary period Δ. Then, we apply the double Wick rotation of the form $t \to i\varphi$, $\varphi \to it$, which yields the line element

$$ds^2_{\text{soliton}} = -r^2 dt^2 + \frac{dr^2}{\frac{r^2}{L^2} - \frac{2\mu_{\text{s}}}{r}} + \left(\frac{r^2}{L^2} - \frac{2\mu_{\text{s}}}{r}\right) d\varphi^2 + r^2 dy^2, \tag{2.2.37}$$

where we have introduced μ_{s} as a new mass parameter for the soliton solution. Notice the profound physical consequence of this algebraic transformation. The

function $f(r) = \frac{r^2}{L^2} - \frac{2\mu_s}{r}$, which previously determined the temporal redshift and the location of the event horizon, now governs the size of the spatial circle parameterized by φ.

As we said, the geometry no longer possesses an event horizon. Instead, as the radial coordinate decreases, the proper size of the φ circle shrinks, eventually collapsing to zero at $r_0 = (2\mu_s L^2)^{1/3}$, where $f(r_0) = 0$. The spacetime simply "caps off" or ends at this radial position.

To ensure this closure is perfectly smooth and free of a conical singularity at the tip, the period Δ can no longer be arbitrary. It must be strictly fixed by the derivative of the metric function evaluated at the tip, requiring

$$\Delta = \frac{4\pi}{f'(r_0)} = \frac{4\pi L^2}{3r_0}. \tag{2.2.38}$$

To establish the global stability of the system, we must compare the free energy densities of the two competing planar geometries. Before doing this, it is useful to recall a simple thermodynamic identity. For a homogeneous thermal state without chemical potentials, the free energy density satisfies

$$\mathcal{F} = \epsilon - Ts = -P, \tag{2.2.39}$$

where ϵ is the energy density, s is the entropy density, and P is the spatial pressure. This relation follows from the Euler relation $\epsilon + P = Ts$, therefore, $\mathcal{F} = -P$.

For the planar Schwarzschild-AdS black hole, the dual state is a conformal fluid in $2+1$ dimensions. The tracelessness of the boundary stress tensor implies

$$-\epsilon + 2P = 0, \tag{2.2.40}$$

so that $\epsilon = 2P$. Combining this with $\epsilon + P = Ts$, we obtain $3P = Ts$, and hence

$$\mathcal{F}_{\text{BH}} = -P = -\frac{1}{3}Ts. \tag{2.2.41}$$

Substituting the planar black hole temperature and entropy density into this relation reproduces (2.2.34). The pressure becomes useful when we pass from

the planar black hole to the AdS soliton. The soliton is obtained by a double Wick rotation, which exchanges the Euclidean time circle with a spatial circle of period Δ. In the boundary theory, this operation exchanges the role of the energy density with the pressure along the compact direction. As a result, the soliton mass density is given by minus the pressure of the corresponding planar black hole configuration,

$$M_{\text{soliton}} = -P_{\text{BH}}. \tag{2.2.42}$$

Since the soliton has no horizon, its classical entropy density vanishes. Therefore, $\mathcal{F}_{\text{soliton}} = M_{\text{soliton}}$. Thus, instead of computing the soliton stress tensor from scratch, we can obtain its free energy density from the black hole result by replacing the thermal scale T_{planar} with the inverse size of the compact spatial circle, $1/\Delta$,

$$\mathcal{F}_{\text{soliton}} = -\frac{32\pi^3}{27}\frac{L^2}{\kappa}\frac{1}{\Delta^3}. \tag{2.2.43}$$

This result reveals that the AdS soliton possesses a negative, constant free energy density that is entirely independent of the temperature.

The global thermodynamic stability of the system is then dictated by the competition between the temperature-dependent $\mathcal{F}_{\text{BH}}(T)$ and the constant $\mathcal{F}_{\text{soliton}}(\Delta)$. By evaluating the coexistence line where a first-order phase transition occurs, $\mathcal{F}_{\text{BH}}(T_c) = \mathcal{F}_{\text{soliton}}(\Delta)$, we simply equate the two expressions

$$-\frac{32\pi^3}{27}\frac{L^2}{\kappa}T_c^3 = -\frac{32\pi^3}{27}\frac{L^2}{\kappa}\frac{1}{\Delta^3} \implies T_c = \frac{1}{\Delta}. \tag{2.2.44}$$

For temperatures $T > T_c$, the planar black hole has a more negative free energy density, making it the globally stable deconfined phase. However, as the temperature drops below T_c, the AdS soliton becomes the absolute minimum of the thermodynamic potential.

2.2.4. Thermodynamic Ensembles and Legendre Transforms

The local thermodynamic stability of a black hole is an intrinsic property that can be fully determined within the microcanonical ensemble, where the black hole is

treated as an isolated system. In this ensemble, the stability is governed entirely by the convexity of the fundamental equation of state, which, in this ensemble, takes the form of the mass expressed as a continuous function of its extensive thermodynamic coordinates: $M = M(S, Q_\Lambda)$.

However, a comprehensive thermodynamic analysis requires exploring the system under different boundary conditions. While the microcanonical ensemble provides a direct framework to assess intrinsic local stability, we are also interested in the behavior of the system when it is allowed to exchange heat and charge with its surroundings. For the charged black holes of the STU model, the grand canonical ensemble serves as the natural generalization. By fixing the intensive variables, specifically, the temperature T and the chemical potentials μ_Λ, this ensemble provides the proper framework to evaluate global phase transitions and competing vacuum states.

Directly calculating the stability bounds in the grand canonical ensemble is often analytically intractable. Conversely, in the planar black holes of the STU Model, the equation of state $M = M(S, Q_\Lambda)$ in the microcanonical ensemble can be found analytically. Our strategy is therefore specific: we compute the stability boundaries in the computationally simpler microcanonical ensemble, and subsequently map those boundaries into the grand canonical ensemble using the properties of Legendre transformations.

In classical black hole thermodynamics, the equation of state $M = M(S, Q_\Lambda)$ completely characterizes the thermal equilibrium of the system by relating all of its extensive thermodynamic coordinates. The First Law dictates the infinitesimal variations of this mass, as

$$dM = TdS + \sum_\Lambda \mu_\Lambda dQ_\Lambda. \tag{2.2.45}$$

From this differential, we can see that the first partial derivatives of the mass with respect to its extensive coordinates simply define the conjugate intensive variables of the system

$$T = \left(\frac{\partial M}{\partial S}\right)_{Q_\Lambda}, \quad \mu_\Lambda = \left(\frac{\partial M}{\partial Q_\Lambda}\right)_{S, Q_{\Gamma \neq \Lambda}}. \tag{2.2.46}$$

As we saw in (2.2.9), for the black hole to remain in stable equilibrium, any physical fluctuation of its extensive coordinates must increase its total energy. If we group the extensive variables into a single vector $x^a = (S, Q_1, Q_2, \dots)$, this local stability requires the second-order variation of the mass to be strictly positive; that is,

$$d^2M = \sum_{a,b} \frac{\partial^2 M}{\partial x^a \partial x^b} dx^a dx^b > 0. \tag{2.2.47}$$

This condition is satisfied if and only if the Hessian matrix of the mass, $\mathcal{H}_{ab} = \partial^2 M / \partial x^a \partial x^b$, is positive-definite. Notice from (2.2.46), that because the first derivatives of the mass yield the intensive variables $y_a = (T, \mu_1, \mu_2, \dots)$, the Hessian matrix acts as the Jacobian matrix that evaluates exactly how the intensive variables react when the extensive coordinates are perturbed

$$\mathcal{H}_{ab} = \frac{\partial y_a}{\partial x^b}. \tag{2.2.48}$$

If this matrix develops a zero eigenvalue (meaning its determinant vanishes), the system reaches a spinodal limit and becomes locally unstable.

To map this microcanonical instability into the grand canonical ensemble, we construct a new thermodynamic potential, the grand potential G, which depends purely on the intensive variables,

$$G(T, \mu_\Lambda) = M - TS - \sum_\Lambda \mu_\Lambda Q_\Lambda. \tag{2.2.49}$$

Taking the total differential of this expression and substituting the First Law (2.2.45), confirms that the differentials of the extensive variables cancel out exactly, as

$$dG = -SdT - \sum_\Lambda Q_\Lambda d\mu_\Lambda. \tag{2.2.50}$$

From this we see that the first derivatives of this new potential return the extensive variables, as $x^a = -\partial G / \partial y_a$.

Now we can see how the physical states of stability map between the two parameter spaces. In the grand canonical ensemble, the response functions of the system, such as the specific heat and the isothermal charge susceptibilities, are encapsulated by the susceptibility matrix χ^{ab}, defined by the second derivatives of the grand potential

$$\chi^{ab} = -\frac{\partial^2 G}{\partial y_a \partial y_b} = \frac{\partial x^a}{\partial y_b}. \tag{2.2.51}$$

We now have two matrices, the microcanonical Hessian $\mathcal{H}_{ab} = \partial y_a / \partial x^b$ and the grand canonical susceptibility $\chi^{ab} = \partial x^a / \partial y_b$. But, according to the inverse function theorem, we know that these two matrices must be related as

$$\chi^{ab} = (\mathcal{H}^{-1})^{ab}, \tag{2.2.52}$$

as long as the transformation is invertible. This fact proves that if the Hessian matrix $\mathcal{H}_{ab}$ develops a zero eigenvalue, its inverse matrix χ^{ab} must necessarily diverge to infinity. Physically, this guarantees that a spinodal point calculated using the computationally simple extensive coordinates corresponds exactly to an infinite divergence in the specific heat or charge susceptibilities of the black hole. Then, we can locate the local stability bounds by evaluating the mass Hessian derived from the equation of state, and subsequently project those exact same physical states into the grand canonical parameter space.

Capítulo 3

Thermodynamics of Planar Black Holes in the STU Model

3.1. Microcanonical Ensemble: The Equation of State and The Hessian

Following the framework established in Chapter 2, our first objective is to find the equation of state in the microcanonical ensemble, where we can determine the local stability of the system. To find the equation of state, we must express the mass parameter m purely in terms of the extensive parameters of the system, as the physical mass is proportional to this parameter, as seen in the asymptotic expansion in 2.1.3. After that, we must evaluate its convexity.

The extensive thermodynamic coordinates of our system are the entropy density and the charge densities. The entropy density S is proportional to the area density of the planar horizon, which is determined by the square root of the determinant of the transverse spatial sector of the metric evaluated at the horizon radius r_0. Hence, up to a numerical factor, the entropy is proportional to the parameter A, which takes the form

$$A = \frac{r_0^2}{L^2}\sqrt{H(r_0)}\,. \tag{3.1.1}$$

The horizon is strictly located at the largest root of the metric function, $f(r_0) = 0$.

For the planar topology, we can algebraically solve for the horizon radius

$$f(r_0) = \frac{L^2}{r_0^2}A^2 - \frac{m}{r_0} - \frac{q}{r_0^2} = 0 \Longrightarrow r_0 = \frac{A^2L^2 - q}{m}. \tag{3.1.2}$$

This can be used to find that

$$H(r_0) = \frac{1}{(A^2L^2 - q)^4}\prod_{\Lambda}\left(A^2L^2 + Q_\Lambda^2\right) = \frac{1}{m^4 r_0^4}\prod_{\Lambda}\left(A^2L^2 + Q_\Lambda^2\right)\ . \tag{3.1.3}$$

When this is replaced in (3.1.1), we obtain the exact, analytical equation of state

$$m = \frac{1}{A^{1/2}L}\prod_{\Lambda}\left(A^2L^2 + Q_\Lambda^2\right)^{1/4}\ . \tag{3.1.4}$$

Because the parameter m is strictly proportional to the total mass density of the system, this relation is the explicit realization of $M = M(S, Q_\Lambda)$. Hence, the condition for local stability is that m is a convex function of the variables $Y^\lambda = (AL, Q_\Lambda)$[1]. The Hessian,

$$\mathcal{H}_{\lambda\sigma} = \frac{\partial^2 m}{\partial Y^\lambda \partial Y^\sigma}\,, \tag{3.1.5}$$

is a 5×5 matrix and the convexity of m is ensured provided all five eigenvalues are strictly non-negative. Once the full analytical Hessian is computed, we restrict our analysis to the T^3 model by evaluating the matrix at $Q_4 = Q_3 = Q_2$. At this point, the determinant simplifies to

$$\det\mathcal{H} = \frac{(A^2L^2 - Q_2^2)^2\,(3A^4L^4 - 2A^2L^2Q_1^2 - Q_1^2Q_2^2)}{64\,A^{9/2}L^7\,(A^2L^2 + Q_1^2)^{3/4}\,(A^2L^2 + Q_2^2)^{9/4}}. \tag{3.1.6}$$

Because of the truncation on the charges, the Hessian exhibits a degenerate spectrum with a repeated eigenvalue, χ, which takes the form

$$\chi = \frac{(A^2L^2 - Q_2^2)(A^2L^2 + Q_1^2)^{1/4}}{2L\sqrt{A}\,(A^2L^2 + Q_2^2)^{5/4}}\,. \tag{3.1.7}$$

For the matrix to be positive-definite, this eigenvalue must be strictly positive

[1]The thermodynamical variables are normalized such that they all have the same dimensions.

($\chi > 0$). This immediately imposes a boundary condition on the physical charges. By defining the dimensionless parameters $\alpha_\Lambda \equiv Q_\Lambda/AL$, which physically represent the charge-to-entropy ratio of the black hole, this first stability constraint reads

$$\alpha_2^2 = \frac{Q_2^2}{A^2L^2} < 1\,. \tag{3.1.8}$$

The other three eigenvalues are solutions of a cubic equation. A necessary condition for the non-negativity of all eigenvalues is that the determinant (3.1.6) is non-negative. By factoring the numerator of the determinant in terms of our dimensionless ratios, this imposes a second, coupled constraint

$$\alpha_1^2 \equiv \frac{Q_1^2}{A^2L^2} < \frac{3}{2+\alpha_2^2}. \tag{3.1.9}$$

We checked that the cubic equation has only real positive roots provided (3.1.8) and (3.1.9) are satisfied. Furthermore, by following the method described in 2.2.1.1, it is possible to show using the Sylvester criterion that the mentioned conditions are sufficient to ensure the positivity of all the principal minors of the Hessian matrix. These conditions are fulfilled by (3.1.8) and (3.1.9), and are given by

$$\begin{gathered}
3\left(A^4L^4 + 2A^2L^2Q_1^2 + Q_1^2Q_2^2\right)\left(A^4L^4 + \left(2A^2L^2 + Q_1^2\right)Q_2^2\right) > 0,\\
3A^6L^6 - A^2L^2Q_1^2Q_2^2 - 2Q_1^2Q_2^4 - 2A^4L^4\left(Q_1^2 - 3Q_2^2\right) > 0,\\
3A^8L^8 - 2A^2L^2Q_1^2Q_2^4 + Q_1^2Q_2^6 - 2A^6L^6\left(Q_1^2 - 2Q_2^2\right) - A^4L^4Q_2^2\left(Q_1^2 + 3Q_2^2\right) > 0,\\
3A^8L^8 + 3Q_1^2Q_2^6 + 2A^6L^6\left(Q_2^2 - Q_1^2\right) - A^4L^4Q_2^2\left(Q_1^2 + 5Q_2^2\right) > 0,\\
\left(A^2L^2 - Q_2^2\right)^2\left(3A^4L^4 - 2A^2L^2Q_1^2 - Q_1^2Q_2^2\right) > 0,
\end{gathered} \tag{3.1.10}$$

The first restriction is always satisfied. In terms of our variables α_1 and α_2, the non-trivial conditions in (3.1.10) are

$$\begin{aligned}
\alpha_1^2 &< \frac{3+6\alpha_2^2}{\alpha_2^2+2\alpha_2^4+2}, \\
\alpha_1^2 &< \frac{3+4\alpha_2^2-3\alpha_2^4}{2\alpha_2^4-\alpha_2^6+2+\alpha_2^2}, \\
\alpha_1^2 &< \frac{3+2\alpha_2^2-5\alpha_2^4}{\alpha_2^2+2-3\alpha_2^6}, \\
\alpha_1^2 &< \frac{3}{2+\alpha_2^2}.
\end{aligned} \tag{3.1.11}$$

The last constraint, which comes from the full 5×5 determinant, is the most restrictive and ultimately defines the stability zone.

We conclude that the stability region is the convex set bounded by the spinodal line of the figure (3.1.1).

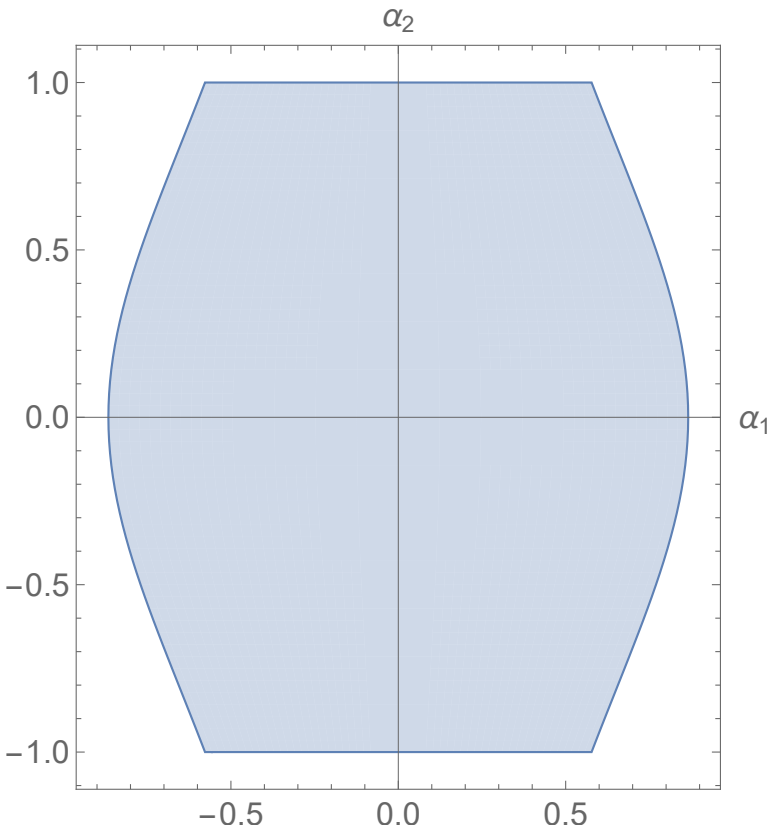

Figura 3.1.1: Stability region of the T^3 model in the microcanonical ensemble.

3.2. Grand Canonical Ensemble

The variational problem in AdS fixes the conformal boundary metric at spacelike infinity. In the Euclidean formulation, this corresponds to fixing the temperature T of the system. We also fix the boundary conditions for the gauge fields, which correspond to fixing the chemical potentials μ_Λ. Studying the phase space of the theory with these boundary conditions corresponds to working in the grand canonical ensemble. We now wish to analytically map the solution space in this ensemble and the spinodal region where the planar black hole configuration ceases to be locally stable.

We continue working within the T^3 model truncation. To construct the grand canonical ensemble, we need to express the mass as a function of the temperature and the chemical potentials μ_Λ. To do this, we introduce intermediate variables (V, Z_Λ) which, after imposing the relevant relations among the parameters of the system, become functions of the temperature and the chemical potentials. We find that, up to overall factors, the physical variables depend on the following ratios

$$\sigma_\Lambda = \frac{\mu_\Lambda}{2\pi T L}\,. \tag{3.2.1}$$

It is possible to eliminate everywhere the harmonic functions $H_\Lambda(r)$ evaluated at the horizon in terms of the other variables using the definition of the chemical potentials,

$$H_\Lambda(r_0) = \frac{Q_\Lambda}{r_0 \mu_\Lambda}\,. \tag{3.2.2}$$

We seek a parametrization that naturally absorbs the temperature and chemical potentials. By postulating Q_Λ to be proportional to a new set of variables Z_Λ scaled by a factor V, we find that a highly useful reparametrization is

$$Q_\Lambda = 2\pi T V L^2 \mu_\Lambda Z_\Lambda\,, \tag{3.2.3}$$

with $q = (2\pi T)^4 V^4 L^6 - m r_0$. The power of this reparametrization becomes immediately useful, as it simplifies the constraint $f(r_0) = 0$ to $Z_1 Z_2^3 = 1$. From the definition of the temperature, T, we can find the mass parameter

$$T = \frac{f'(r_0)}{4\pi H(r_0)^{1/2}} \implies m = L^4(2\pi T)^3 \left(Z_2^2(Z_2+3Z_1)V - 2\right) V^2. \tag{3.2.4}$$

The equations $Q_\Lambda^2 - q_\Lambda m + q = 0$ are rewritten using our reparametrization as

$$3V^2 Z_1^2 Z_2^2 - 2V Z_1 - \sigma_1^2 Z_1^2 = 0\,, \tag{3.2.5}$$

$$V^2 Z_2^4 + 2V^2 - 2V Z_2 - \sigma_2^2 Z_2^2 = 0\,. \tag{3.2.6}$$

Equations (3.2.5) and (3.2.6) can be combined to yield a linear equation for the variable V, which allows us to find

$$V = -\frac{1}{2}\,\frac{\sigma_1^2 Z_2^4 + 2\sigma_1^2 - 3Z_2^4\sigma_2^2}{Z_2^3(Z_2^4-1)}\,. \tag{3.2.7}$$

Given (3.2.7), (3.2.5) and (3.2.6) imply that

$$4Z_2^{12}\sigma_2^2 + \left(6\sigma_1^2\sigma_2^2 - \sigma_1^4 - 9\sigma_2^4 - 4\sigma_1^2 - 4\sigma_2^2\right) Z_2^8 - 4\sigma_1^2\left(-3\sigma_2^2 + \sigma_1^2 - 1\right) Z_2^4 - 4\sigma_1^4 = 0\,. \tag{3.2.8}$$

The cubic equation for Z_2^4 (3.2.8), indicates that there is at most 3 solutions for every value of the boundary conditions parameterized by (σ_1, σ_2).

3.2.1. Mapping The Stability Region

To find the stability region for the variables in the grand canonical ensemble we notice that the variables that dictated the stability region in the microcanonical ensemble are related to the (σ_1, σ_2) variables through our intermediate variables V, Z_1 and $Z2$, notice that

$$\alpha_2 = \frac{Q_2}{AL} = \sigma_2 \frac{Z_2}{V}\,. \tag{3.2.9}$$

Hence, we introduce the change of variables

$$\sigma_2 = \nu_2 \frac{V}{Z_2}\,, \tag{3.2.10}$$

with $\nu_2 \in (-1, 1)$ to ensure the condition of stability (3.1.8). The other charge has a similar parametrization

$$\alpha_1 = \frac{Q_1}{AL} = \frac{\sigma_1}{V Z_2^3}\,. \tag{3.2.11}$$

The following change of parameters

$$\sigma_1 = \frac{\sqrt{3}}{\sqrt{2+\nu_2^2}}\,\nu_1 V Z_2^3\,, \tag{3.2.12}$$

enforces the second condition of stability, (3.1.9), provided $\nu_1 \in (-1, 1)$. If we replace (3.2.10) and (3.2.12) in (3.2.5) and (3.2.6) we get

$$Z_2^4 = \frac{\nu_2^4 + 2 + 3\nu_2^2}{2 + 3\nu_1^2 + \nu_2^2}\,, \tag{3.2.13}$$

$$V = -\frac{2}{3}\frac{Z_2(2+\nu_2^2)}{\nu_1^2 Z_2^4 - 2 - \nu_2^2}\,. \tag{3.2.14}$$

We use (3.2.13) and (3.2.14) to have the explicit form of (σ_1, σ_2) in terms of the quantities bounded by the stability conditions, ν_Λ. The result is

$$\sigma_1 = -\frac{2}{3}\frac{\sqrt{3}\sqrt{2+\nu_2^2}\,\nu_1\,(\nu_2^2+1)}{-\nu_2^2 + \nu_2^2\nu_1^2 - 2 - 2\nu_1^2}\,, \tag{3.2.15}$$

$$\sigma_2 = -\frac{2}{3}\frac{(2 + 3\nu_1^2 + \nu_2^2)\,\nu_2}{-\nu_2^2 + \nu_2^2\nu_1^2 - 2 - 2\nu_1^2} \tag{3.2.16}$$

The boundary conditions that yield stable black holes correspond to the shaded region shown in the figure (3.2.1). We note that this analysis yields a relatively simple parametric solution to the cubic equation (3.2.8).

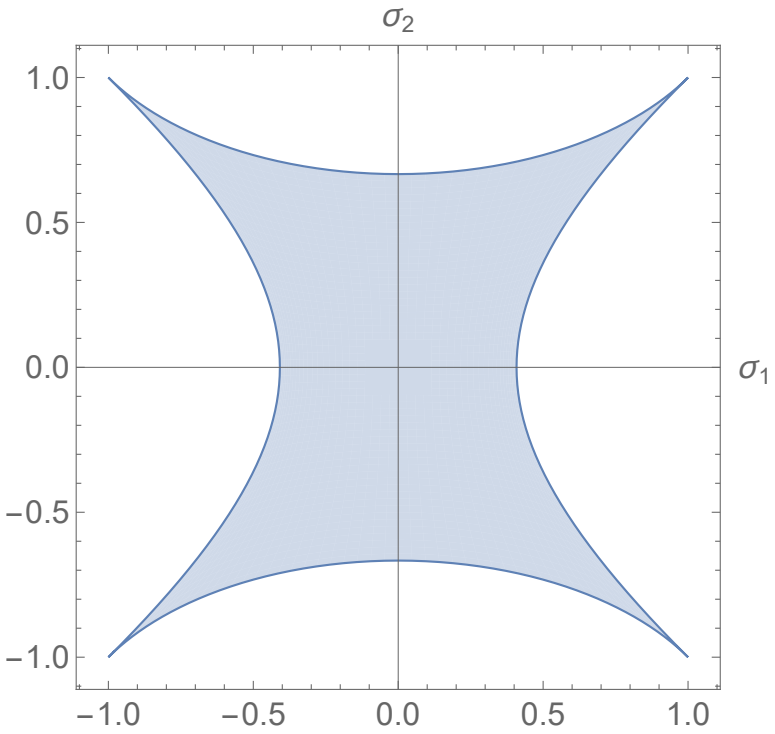

Figura 3.2.1: Boundary conditions that yield stable black holes in the T^3 model.

3.3. The space of solutions

3.3.1. Black Holes

Now that we have the locally stable solutions, we are interested in their characterization by their free energy. Hence, we wish to plot the Gibbs free energy density $\frac{L^2}{\kappa}\omega$ versus σ_Λ. Notice that this is the analog of the free energy (or free energy density) G in the grand canonical ensemble which we treated in our theoretical framework. The standard thermodynamical relations allow a straightforward calculation. Indeed,

$$\omega = -\frac{\kappa}{L^2}P = -\frac{m}{2L^4} = -\frac{1}{2}(2\pi T)^3\left(Z_2^2(Z_2+3Z_1)V-2\right)V^2\,. \tag{3.3.1}$$

where P is the pressure of the dual fluid given in (2.1.40), as we saw in 2.2.3. It is enlightening to graph the dimensionless free energy $\omega_0 = \frac{\omega}{(2\pi T)^3}$ vs (σ_1, σ_2), which can be seen in figure (3.3.1). We learn that stable thermal states exist for $\omega_0 \in [-1, -\frac{4}{27}]$.

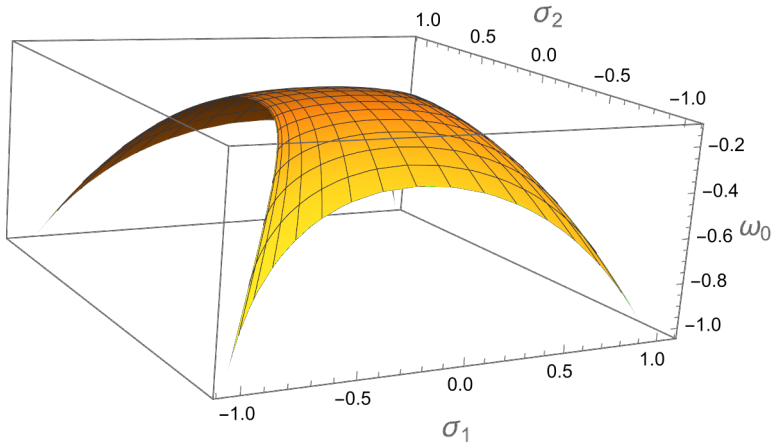

Figura 3.3.1: Free energy density of the stable black holes of the T^3 model in the grand canonical ensemble. Stable thermal states exist for $\omega_0 \in [-1, -\frac{4}{27}]$.

3.3.2. AdS Solitons

As explained in Chapter 2, if the metric of the conformal boundary has a compact direction, $\varphi \in [0, \Delta]$, there exist solitons that have the same boundary conditions as the black holes. These solitons are in equilibrium with arbitrary chemical potentials because loops around the time direction are non-contractible, and therefore time is a globally defined coordinate. These solutions are described in detail in [29]. The solution space is characterized by the quantities

$$\psi_1 = \frac{1}{2\pi L} \lim_{r\to\infty} \oint A^1_\varphi \, \mathrm{d}\varphi \,, \qquad \psi_2 = \frac{1}{2\pi L} \lim_{r\to\infty} \oint A^2_\varphi \, \mathrm{d}\varphi \,. \tag{3.3.2}$$

These are called Wilson Loops. With the energy density $\frac{L^2}{\kappa}\epsilon_{\text{sol}}$ [2], which also describes their Gibbs free energy, given by

$$\epsilon_{\text{sol}} = \pm \frac{2\pi^3}{\Delta^3} \, x_0 \, \left|2x_0^2\psi_1^2 + \psi_1^2 - 3\psi_2^2\right| \, \frac{\psi_1^2 x_0^4 - \psi_2^2}{(x_0^2-1)^2} \tag{3.3.3}$$

where the + sign is for solutions with $x_0 > 1$ and the − sign is for solutions with $x_0 < 1$. The parameter x_0 denotes the radial position of the tip of the soliton geometry, namely the point where the compact φ circle smoothly contracts in the interior. Equivalently, it is determined by the regularity condition $f(x_0) = 0$ in the soliton metric of [29]. The solutions are the roots of the polynomial

[2] Note that $\psi_1^{\text{Here}} = \sqrt{2}\,\psi_1^{\text{There}}$ and $\psi_2^{\text{Here}} = \sqrt{\frac{2}{3}}\,\psi_2^{\text{There}}$ where "There" are the variables of [29].

$$4\psi_1^4 x_0^6+4\psi_1^2(\psi_1^2-3\psi_2^2+1)x_0^4+(\psi_1^4-6\psi_1^2\psi_2^2-4\psi_1^2-4\psi_2^2+9\psi_2^4)x_0^2+4\psi_2^2=0. \quad (3.3.4)$$

Inspired by the parametric solution of the equation for the existence of black holes (3.2.8), we found the following simple parametric solution of the equation (3.3.4),

$$x_0 = \frac{\cosh\xi_2}{\cosh\xi_1}\,, \quad (3.3.5)$$

$$\psi_1 = \frac{\sinh 2\xi_1}{\cosh{\xi_1}^2+3\cosh{\xi_2}^2-1}\,, \quad (3.3.6)$$

$$\psi_2 = \frac{\sinh 2\xi_2}{\cosh{\xi_1}^2+3\cosh{\xi_2}^2-1}\,. \quad (3.3.7)$$

When (3.3.6) and (3.3.7) are replaced in the equation (3.3.4), it factorizes. In addition to the solution (3.3.5) we find that there is always another solution with $x_0^2 > 0$. Therefore, there are two soliton solutions at each value of the boundary conditions (ψ_1, ψ_2). The set of boundary conditions that yield these solutions can be seen in figure (3.3.2). There is also a branch of solitons with positive energy that is not relevant for the possible phase transitions with the black holes, as the free energy of the black holes is always negative, a plot of the free energy density of these solitons can be seen in 3.3.3.

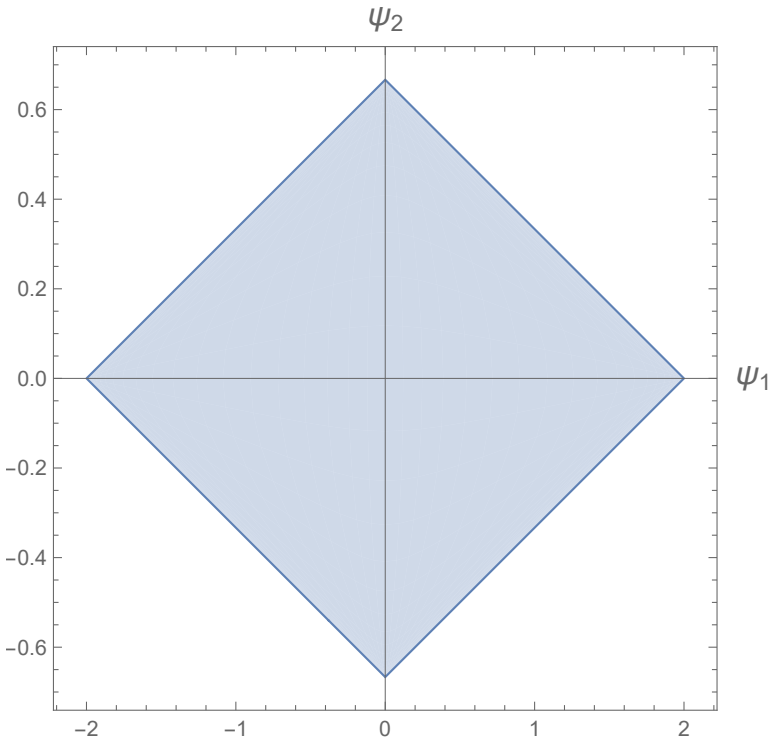

Figura 3.3.2: The boundary conditions that yield solitons for the T^3 model.

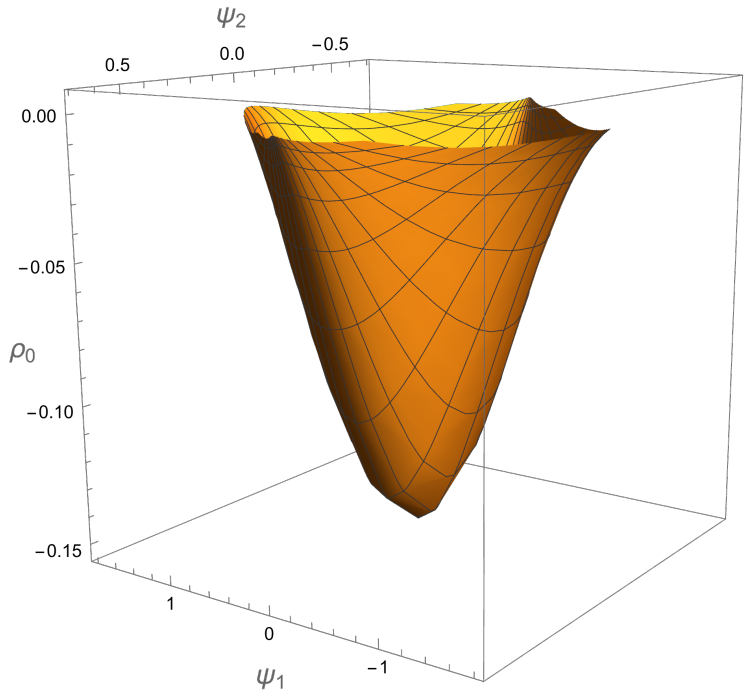

Figura 3.3.3: Energy density of the branch of solitons with negative energy. We plot $\epsilon_0 = \frac{\Delta^3}{(2\pi)^3}\epsilon_{\text{sol}} \in [-\frac{4}{27}, 0]$. The solutions at $\epsilon_0 = 0$ are supersymmetric.

Capítulo 4

First Order Phase Transition

As established in our theoretical framework, the global thermodynamic stability of the planar system is dictated by the competition between the planar black hole and the AdS soliton. In the grand canonical ensemble of the T^3 model, their respective free energy densities are given by ω for the black hole and ϵ_{sol} for the soliton. The black hole free energy can be written as

$$\omega = (2\pi T)^3 \omega_0, \qquad \omega_0 < 0, \tag{4.0.1}$$

while the soliton free energy is temperature independent and scales with the size of the compact circle as

$$\epsilon_{\text{sol}} = \frac{(2\pi)^3}{\Delta^3}\epsilon_0, \qquad \epsilon_0 < 0. \tag{4.0.2}$$

A first-order phase transition occurs at the coexistence line where these free energies are exactly equal

$$\omega = \epsilon_{\text{sol}} \implies T^3\Delta^3 = \frac{\epsilon_0}{\omega_0}\,. \tag{4.0.3}$$

Since both ω_0 and ϵ_0 are negative, the ratio ϵ_0/ω_0 is positive. The dominant phase is the one with the lower, more negative, free energy. Therefore, for

$$T^3\Delta^3 > \frac{\epsilon_0}{\omega_0}\,, \tag{4.0.4}$$

the planar black hole dominates, as expected from the scaling $\omega \sim -T^3$ at high temperature. Conversely, for

$$T^3\Delta^3 < \frac{\epsilon_0}{\omega_0}\,, \tag{4.0.5}$$

the AdS soliton has the lower free energy and becomes the thermodynamically preferred saddle. This transition is first order because the entropy density jumps from the finite black hole value to the strictly vanishing on the soliton.

For fixed Wilson loops (ψ_1, ψ_2), the soliton equation can admit more than one positive root for x_0^2. These roots correspond to distinct soliton branches satisfying the same boundary conditions, with x_0 denoting the position of the tip where the compact circle closes off. The labels $x_0 > 1$ and $x_0 < 1$ distinguish the two possible radial domains of the soliton geometry. In the phase comparison, the relevant soliton is the branch with the lowest free energy among the branches allowed by the same boundary data.

A useful consistency check is obtained by switching off the spatial Wilson loops, $\psi_1 = \psi_2 = 0$. In this limit the soliton sector reduces to the usual neutral AdS soliton discussed in the theoretical framework, namely the double Wick rotation of the planar Schwarzschild-AdS black hole. The relevant saddle is then the neutral soliton, whose normalized free energy is $\epsilon_0 = -4/27$. This point is the lower endpoint of the negative-energy soliton branch. Notice that the polynomial equation for x_0^2 becomes degenerate at $\psi_1 = \psi_2 = 0$, so this case should be understood as the neutral AdS soliton limit rather than as a generic point with multiple soliton roots. Since the corresponding neutral planar black hole has $\omega_0 = -4/27$, the coexistence condition gives $T_c\Delta = 1$, reproducing the standard transition. Therefore, the comparison between charged dilatonic black holes and solitons presented here contains the Schwarzschild-AdS result as the zero-Wilson-line limit, the non-zero Wilson loops describe the genuine extension to the charged STU sector.

Solitonic preemption of the spinodal region

The coexistence equation should be interpreted at fixed boundary geometry. The period Δ is not a thermodynamic variable of a given ensemble, but an external geometric modulus that fixes the size of the compact spatial circle on which the boundary theory is defined. For a prescribed value of Δ, the equation

$$T_c^3 \Delta^3 = \frac{\epsilon_0}{\omega_0} \tag{4.0.6}$$

determines the critical temperature T_c at which the black hole and the soliton exchange dominance. Conversely, one may scan the family of boundary theories obtained by varying the compactification scale Δ. This allows us to ask for which values of Δ the solitonic first-order transition occurs before the black hole reaches the boundary of local thermodynamic stability.

Let $T_{\rm ins}$ denote the temperature at which a black hole reaches one of the spinodal curves. The critical compactification scale is defined by imposing that the coexistence temperature coincides with the instability temperature. Thus,

$$\Delta_{\rm crit} = \frac{1}{T_{\rm ins}} \left(\frac{\epsilon_0^{\rm min}}{\omega_0(\nu_i^2 = 1)} \right)^{1/3} . \tag{4.0.7}$$

Here $\epsilon_0^{\rm min}$ is obtained by solving the soliton regularity equation for the allowed positive roots of x_0^2 at fixed Wilson loops (ψ_1, ψ_2), evaluating the normalized soliton free energy on each physical branch, and selecting the lowest value. The notation $\omega_0(\nu_i^2 = 1)$ means that the black hole free energy is evaluated on the corresponding spinodal curve. Since both $\epsilon_0^{\rm min}$ and ω_0 are negative, the ratio in (4.0.7) is positive. The scale $\Delta_{\rm crit}$ is therefore fixed entirely by boundary data, through the instability temperature determined by the chemical potentials and through the soliton energy determined by the Wilson loops.

The physical interpretation is then straightforward when the system is cooled from high temperature. For $\Delta < \Delta_{\rm crit}$, the transition temperature satisfies $T_c > T_{\rm ins}$, so the soliton becomes globally dominant before the black hole loses local stability. For $\Delta = \Delta_{\rm crit}$, the first-order transition occurs exactly at the spinodal curve. For $\Delta > \Delta_{\rm crit}$, the black hole reaches local instability before the soliton becomes the dominant saddle. In that regime, within the space of homogeneous black holes and solitons considered here, the local instability has no thermodynamic resolution.

The endpoint of the system is then an open question, possibly involving solutions outside the present ansatz or genuinely out-of-equilibrium dynamics.

There are two relevant boundary cases:

Case 1: $\nu_2^2 = 1$.

At this stability bound, the dimensionless free energy of the black hole evaluates to

$$\omega_0(\nu_2^2 = 1) = -\frac{8\sqrt{6}}{27}\frac{(3+3\nu_1^2)^{5/2}}{(\nu_1^2+3)^3}. \tag{4.0.8}$$

On this curve, the boundary variables reduce to

$$\sigma_1 = \frac{4\nu_1}{\nu_1^2+3}, \qquad \sigma_2 = \frac{2(\nu_1^2+1)}{\nu_1^2+3}. \tag{4.0.9}$$

Using $\sigma_\Lambda = \mu_\Lambda/(2\pi TL)$, the instability temperature may be written as

$$T_{\text{ins}}^{(1)} = \frac{\mu_1(\nu_1^2+3)}{8\pi L\nu_1}. \tag{4.0.10}$$

Equivalently,

$$T_{\text{ins}}^{(1)} = \frac{\mu_2(\nu_1^2+3)}{4\pi L(\nu_1^2+1)}. \tag{4.0.11}$$

These two expressions describe the same point on the spinodal curve when the chemical potentials obey

$$\frac{\mu_2}{\mu_1} = \frac{\nu_1^2+1}{2\nu_1}. \tag{4.0.12}$$

The corresponding critical compactification scale is therefore

$$\Delta_{\text{crit}}^{(1)} = \frac{1}{T_{\text{ins}}^{(1)}}\left(\frac{\epsilon_0^{\min}}{\omega_0(\nu_2^2=1)}\right)^{1/3}. \tag{4.0.13}$$

Case 2: $\nu_1^2 = 1$

Similarly, at the second stability bound, the free energy becomes

$$\omega_0(\nu_1^2 = 1) = -\frac{1}{432}(5+\nu_2^2)^{5/2}(2+\nu_2^2)^{1/2}(\nu_2^2+1)^{3/2}. \tag{4.0.14}$$

On this curve, the boundary variables become

$$\sigma_1 = \frac{\nu_2^2+1}{6}\sqrt{3\nu_2^2+6}, \qquad \sigma_2 = \frac{\nu_2(\nu_2^2+5)}{6}. \tag{4.0.15}$$

The instability temperature may be written as

$$T_{\text{ins}}^{(2)} = \frac{3\mu_1}{\pi L(\nu_2^2+1)\sqrt{3\nu_2^2+6}}. \tag{4.0.16}$$

Equivalently,

$$T_{\text{ins}}^{(2)} = \frac{3\mu_2}{\pi L\nu_2(\nu_2^2+5)}. \tag{4.0.17}$$

These two expressions describe the same point on the spinodal curve when

$$\frac{\mu_2}{\mu_1} = \frac{\nu_2(\nu_2^2+5)}{(\nu_2^2+1)\sqrt{3\nu_2^2+6}}. \tag{4.0.18}$$

The corresponding critical compactification scale is

$$\Delta_{\text{crit}}^{(2)} = \frac{1}{T_{\text{ins}}^{(2)}}\left(\frac{\epsilon_0^{\min}}{\omega_0(\nu_1^2=1)}\right)^{1/3}. \tag{4.0.19}$$

The resulting phase structure is controlled by the compactification scale. For each spinodal branch, Δ_{crit} separates compactifications where the solitonic phase becomes dominant before the black hole reaches local instability from compactifications where the homogeneous black hole reaches the spinodal curve first. Thus, the charged planar system admits a standard black hole to soliton first-order transition in the range $\Delta \leq \Delta_{\text{crit}}$, while the regime $\Delta > \Delta_{\text{crit}}$ points to the possible relevance of additional classical saddles in the global phase diagram.

Capítulo 5

Conclusions

Conclusiones

En este trabajo, hemos estudiado la estabilidad local y global de soluciones de agujeros negros planos cargados en el contexto del modelo STU, una truncación consistente de la supergravedad gauged $\mathcal{N} = 8$. Al enfocarnos en el sector T^3, redujimos la complejidad de la teoría maximal a un modelo tratable que involucra un único dilatón efectivo acoplado a dos cargas de gauge independientes. Esto permitió realizar un mapeo exhaustivo del espacio de parámetros, conectando las soluciones gravitacionales exactas con su interpretación termodinámica en la teoría de campos dual.

Hemos mostrado que:

- La estabilidad microcanónica está acotada por razones de carga específicas: La estabilidad local de estos agujeros negros no está garantizada en todas las regiones del espacio de parámetros. Al analizar el Hessiano del parámetro de masa m, identificamos que la estabilidad se mantiene únicamente dentro de una región convexa acotada por las condiciones $\alpha_2^2 < 1$ y $\alpha_1^2 < 3/(2 + \alpha_2^2)$.
- El solitón es un saddle competitivo para topologías planas con una dirección compacta: Para el caso de horizontes planos, el solitón de AdS, obtenido mediante una doble rotación de Wick, debe ser incluido en la comparación termodinámica siempre que la teoría de borde se formule sobre un círculo espacial de periodo Δ. Debido a que el solitón posee una coordenada temporal

globalmente definida, puede existir en equilibrio con potenciales químicos arbitrarios μ_Λ y proporciona el candidato natural al vacío confinante.

Además, mostramos que la competencia entre el agujero negro planar y el solitón de AdS generaliza la transición de confinamiento-deconfinamiento del caso planar neutro. En particular, cuando se apagan los Wilson loops espaciales, el análisis recupera la transición estándar entre el black brane de Schwarzschild-AdS y el solitón de Horowitz-Myers, con $T_c\Delta = 1$. En presencia de cargas y Wilson loops, la condición de coexistencia se deforma y determina una temperatura crítica que depende de la rama solitónica dominante.

El análisis también identifica el papel del periodo Δ como un módulo geométrico externo que fija la compactificación espacial de la teoría de borde. Al considerar la familia de teorías compactificadas con distintos tamaños de círculo, las curvas espinodales permiten definir una escala crítica Δ_{crit} determinada completamente por datos de borde: la temperatura de inestabilidad, fijada por los potenciales químicos μ_Λ, y la energía de la rama solitónica dominante, fijada por los Wilson loops ψ_Λ. Para compactificaciones con $\Delta \leq \Delta_{\text{crit}}$, la transición de primer orden hacia el solitón ocurre antes o justo cuando el agujero negro pierde estabilidad local. Para $\Delta > \Delta_{\text{crit}}$, dentro del espacio de agujeros negros homogéneos y solitones considerado en esta tesis, la inestabilidad local aparece antes de que el solitón sea globalmente dominante.

Finalmente, los resultados de esta tesis muestran que incluir campos escalares, múltiples cargas y módulos geométricos de compactificación conduce a una estructura de fases mucho más rica y compleja. Los límites de estabilidad, las superficies de coexistencia y la escala Δ_{crit} proporcionan una base clara para estudiar configuraciones más generales. En particular, el régimen $\Delta > \Delta_{\text{crit}}$ señala una dirección natural para trabajos futuros, donde la completación del diagrama de fases podría requerir soluciones fuera del ansatz homogéneo o una descripción

dinámica fuera del equilibrio.

Conclusions

In this work, we have studied the local and global stability of charged planar black hole solutions in the context of the STU model, a consistent truncation of gauged $\mathcal{N} = 8$ supergravity. By focusing on the T^3 sector, we reduced the complexity of the maximal theory to a tractable model involving a single effective dilaton coupled to two independent gauge charges. This allowed for a comprehensive mapping of the parameter space, bridging the gap between exact gravitational solutions and their thermodynamic interpretation in the dual field theory.

We have shown that:

- Microcanonical Stability is bounded by specific charge ratios: The local stability of these black holes is not guaranteed for all regions of the parameter space. By analyzing the Hessian of the mass parameter m, we identified that stability is maintained only within a convex region bounded by the conditions $\alpha_2^2 < 1$ and $\alpha_1^2 < 3/(2 + \alpha_2^2)$.
- The soliton is a competing saddle for planar topologies with a compact direction: For planar horizons, the AdS soliton, obtained via a double Wick rotation, must be included in the thermodynamic comparison whenever the boundary theory is placed on a spatial circle of period Δ. Because the soliton possesses a globally defined time coordinate, it can exist in equilibrium with arbitrary chemical potentials μ_Λ and provides the natural candidate for the confining vacuum.

Additionally, we showed that the competition between the planar black hole and the AdS soliton generalizes the confinement-deconfinement transition of the neutral planar case. In particular, when the spatial Wilson loops are turned off, the analysis recovers the standard transition between the Schwarzschild-AdS black brane and the Horowitz-Myers soliton, with $T_c\Delta = 1$. In the presence of charges and Wilson loops, the coexistence condition is deformed and determines a critical temperature that depends on the dominant soliton branch.

The analysis also identifies the role of the period Δ as an external geometric modulus fixing the spatial compactification of the boundary theory. By considering the family of compactified theories with different circle sizes, the spinodal curves define a critical scale Δ_{crit} completely determined by boundary data: the instability

temperature, fixed by the chemical potentials μ_Λ, and the energy of the dominant soliton branch, fixed by the Wilson loops ψ_Λ. For compactifications with $\Delta \leq \Delta_{\text{crit}}$, the first-order transition to the soliton occurs before or exactly when the black hole loses local stability. For $\Delta > \Delta_{\text{crit}}$, within the space of homogeneous black holes and solitons considered in this thesis, the local instability appears before the soliton becomes globally dominant.

Finally, the results of this thesis show that including scalar fields, multiple charges, and geometric compactification moduli leads to a much richer and more complex phase structure. The stability bounds, coexistence surfaces, and the scale Δ_{crit} provide a clear foundation for studying more general configurations. In particular, the regime $\Delta > \Delta_{\text{crit}}$ points to a natural direction for future work, where completing the phase diagram may require solutions outside the homogeneous ansatz or a genuinely out-of-equilibrium dynamical description.

Bibliografía

[1] Juan Martin Maldacena. The Large N limit of superconformal field theories and supergravity. *Adv. Theor. Math. Phys.*, 2:231–252, 1998. doi: 10.4310/ATMP.1998.v2.n2.a1.

[2] S.S. Gubser, I.R. Klebanov, and A.M. Polyakov. Gauge theory correlators from non-critical string theory. *Physics Letters B*, 428(1-2):105–114, May 1998. ISSN 0370-2693. doi: 10.1016/s0370-2693(98)00377-3. URL http://dx.doi.org/10.1016/S0370-2693(98)00377-3.

[3] Edward Witten. Anti de Sitter space and holography. *Adv. Theor. Math. Phys.*, 2:253–291, 1998. doi: 10.4310/ATMP.1998.v2.n2.a2.

[4] Ofer Aharony, Steven S. Gubser, Juan Martin Maldacena, Hirosi Ooguri, and Yaron Oz. Large N field theories, string theory and gravity. *Phys. Rept.*, 323: 183–386, 2000. doi: 10.1016/S0370-1573(99)00083-6.

[5] Edward Witten. Anti-de Sitter space, thermal phase transition, and confinement in gauge theories. *Adv. Theor. Math. Phys.*, 2:505–532, 1998. doi: 10.4310/ATMP.1998.v2.n3.a3.

[6] P. K. Kovtun, D. T. Son, and A. O. Starinets. Viscosity in strongly interacting quantum field theories from black hole physics. *Phys. Rev. Lett.*, 94:111601, Mar 2005. doi: 10.1103/PhysRevLett.94.111601. URL https://link.aps.org/doi/10.1103/PhysRevLett.94.111601.

[7] S. W. Hawking and Don N. Page. Thermodynamics of Black Holes in anti-De Sitter Space. *Commun. Math. Phys.*, 87:577, 1983. doi: 10.1007/BF01208266.

[8] Sumati Surya, Kristin Schleich, and Donald M. Witt. Phase transitions for flat AdS black holes. *Phys. Rev. Lett.*, 86:5231–5234, 2001. doi: 10.1103/PhysRevLett.86.5231.

[9] Tatsuma Nishioka, Shinsei Ryu, and Tadashi Takayanagi. Holographic Superconductor/Insulator Transition at Zero Temperature. *JHEP*, 03:131, 2010. doi: 10.1007/JHEP03(2010)131.

[10] Gary T. Horowitz and Benson Way. Complete Phase Diagrams for a Holographic Superconductor/Insulator System. *JHEP*, 11:011, 2010. doi: 10.1007/JHEP11(2010)011.

[11] Andrés Anabalón, Patrick Concha, Julio Oliva, Constanza Quijada, and Evelyn Rodríguez. Phase transitions for charged planar solitons in AdS. *Phys. Lett. B*, 835:137521, 2022. doi: 10.1016/j.physletb.2022.137521.

[12] Constanza Quijada, Andrés Anabalón, Robert B. Mann, and Julio Oliva. Triple points of gravitational AdS solitons and black holes. *Phys. Rev. D*, 110 (2):L021902, 2024. doi: 10.1103/PhysRevD.110.L021902.

[13] M. J. Duff and James T. Liu. Anti-de Sitter black holes in gauged N = 8 supergravity. *Nucl. Phys. B*, 554:237–253, 1999. doi: 10.1016/S0550-3213(99)00299-0.

[14] Mirjam Cvetic and Steven S. Gubser. Phases of R charged black holes, spinning branes and strongly coupled gauge theories. *JHEP*, 04:024, 1999. doi: 10.1088/1126-6708/1999/04/024.

[15] Mirjam Cvetic and Steven S. Gubser. Thermodynamic stability and phases of general spinning branes. *JHEP*, 07:010, 1999. doi: 10.1088/1126-6708/1999/07/010.

[16] Steven S. Gubser and Indrajit Mitra. Instability of charged black holes in Anti-de Sitter space. *Clay Math. Proc.*, 1:221, 2002.

[17] Steven S. Gubser and Indrajit Mitra. The Evolution of unstable black holes in anti-de Sitter space. *JHEP*, 08:018, 2001. doi: 10.1088/1126-6708/2001/08/018.

[18] Oscar Henriksson, Carlos Hoyos, and Niko Jokela. Novel color superconducting phases of $\mathcal{N} = 4$ super Yang-Mills at strong coupling. *JHEP*, 09:088, 2019. doi: 10.1007/JHEP09(2019)088.

[19] Liam Gladden, Victor Ivo, Pavel Kovtun, and Andrei O. Starinets. Instability in N=4 supersymmetric Yang-Mills theory at finite density. *Phys. Rev. D*, 111(8):086030, 2025. doi: 10.1103/PhysRevD.111.086030.

[20] Marcelo Andrés Oyarzo Catalán. *Black Holes and Solitons in String Theory and M-Theory*. PhD thesis, Concepcion U., 2025.

[21] Andrés Anabalón, Stefano Maurelli, Marcelo Oyarzo, and Mario Trigiante. The instability of low-temperature black holes in gauged $\mathcal{N} = 8$ supergravity. *JHEP*, 03:201, 2025. doi: 10.1007/JHEP03(2025)201.

[22] Andrés Anabalón, Mariano Chernicoff, Gaston Giribet, Julio Oliva, and Martín Reyes. Quark-Antiquark Potential as a Probe for Holographic Phase Transitions. *arXiv preprint arXiv:2501.15533*, 1 2025.

[23] Alex Buchel. Instability of baryonic black branes. *JHEP*, 05:215, 2025. doi: 10.1007/JHEP05(2025)215.

[24] Alex Buchel. On the relevance of GIKS instability of charged N=4 SYM plasma. *arXiv preprint arXiv:2502.11354*, 2 2025.

[25] Liam Gladden, Victor Ivo, Pavel K. Kovtun, and Andrei O. Starinets. Hydrodynamics with multiple charges and holography. *arXiv preprint arXiv:2507.21346*, 7 2025.

[26] Andres Anabalon and Julio Oliva. Plasma-Plasma Third Order Phase Transition from Type IIB Supergravity. *Phys. Rev. Lett.*, 133(12):121601, 2024. doi: 10.1103/PhysRevLett.133.121601.

[27] Oscar J. C. Dias, Prahar Mitra, and Jorge E. Santos. Charged rotating hairy black holes in $AdS_5 \times S^5$: unveiling their secrets. *JHEP*, 06:051, 2025. doi: 10.1007/JHEP06(2025)051.

[28] Andres Anabalon and Simon F. Ross. Supersymmetric solitons and a degeneracy of solutions in AdS/CFT. *JHEP*, 07:015, 2021. doi: 10.1007/JHEP07(2021)015.

[29] Andrés Anabalón, Antonio Gallerati, Simon Ross, and Mario Trigiante. Supersymmetric solitons in gauged $\mathcal{N} = 8$ supergravity. *JHEP*, 02:055, 2023. doi: 10.1007/JHEP02(2023)055.

[30] Andres Anabalon, Mattia Cesaro, Antonio Gallerati, Alfredo Giambrone, and Mario Trigiante. A positive energy theorem for AdS solitons. *Phys. Lett. B*, 846:138226, 2023. doi: 10.1016/j.physletb.2023.138226.

[31] A. Anabalón, D. Astefanesei, A. Gallerati, and J. Oliva. Supersymmetric smooth distributions of M2-branes as AdS solitons. *JHEP*, 05:077, 2024. doi: 10.1007/JHEP05(2024)077.

[32] Andrés Anabalón, Horatiu Nastase, and Marcelo Oyarzo. Supersymmetric AdS solitons and the interconnection of different vacua of $\mathcal{N} = 4$ Super Yang-Mills. *JHEP*, 05:217, 2024. doi: 10.1007/JHEP05(2024)217.

[33] Gary T. Horowitz and Robert C. Myers. The AdS / CFT correspondence and a new positive energy conjecture for general relativity. *Phys. Rev. D*, 59: 026005, 1998. doi: 10.1103/PhysRevD.59.026005.

[34] Carlos Nunez, Marcelo Oyarzo, and Ricardo Stuardo. Confinement and D5-branes. *JHEP*, 03:080, 2024. doi: 10.1007/JHEP03(2024)080.

[35] Ali Fatemiabhari and Carlos Nunez. From conformal to confining field theories using holography. *JHEP*, 03:160, 2024. doi: 10.1007/JHEP03(2024)160.

[36] Dimitrios Chatzis, Ali Fatemiabhari, Carlos Nunez, and Peter Weck. Conformal to confining SQFTs from holography. *JHEP*, 08:041, 2024. doi: 10.1007/JHEP08(2024)041.

[37] Dimitrios Chatzis, Ali Fatemiabhari, Carlos Nunez, and Peter Weck. SCFT deformations via uplifted solitons. *Nucl. Phys. B*, 1006:116659, 2024. doi: 10.1016/j.nuclphysb.2024.116659.

[38] Mauro Giliberti, Ali Fatemiabhari, and Carlos Nunez. Confinement and

screening via holographic Wilson loops. *JHEP*, 11:068, 2024. doi: 10.1007/JHEP11(2024)068.

[39] Federico Castellani and Carlos Nunez. Holography for confined and deformed theories: TsT-generated solutions in type IIB supergravity. *JHEP*, 12:155, 2024. doi: 10.1007/JHEP12(2024)155.

[40] Niall T. Macpherson, Paul Merrikin, and Ricardo Stuardo. Circle compactifications of Minkowski$_D$ solutions, flux vacua and solitonic branes. *JHEP*, 08:143, 2025. doi: 10.1007/JHEP08(2025)143.

[41] Marcelo Barbosa, Horatiu Nastase, Carlos Nunez, and Ricardo Stuardo. Penrose limits of I-branes, twist-compactified D5-branes, and spin chains. *Phys. Rev. D*, 110(4):046015, 2024. doi: 10.1103/PhysRevD.110.046015.

[42] Carlos Nunez, Marcelo Oyarzo, and Ricardo Stuardo. Confinement in (1 + 1) dimensions: a holographic perspective from I-branes. *JHEP*, 09:201, 2023. doi: 10.1007/JHEP09(2023)201.

[43] Ali Fatemiabhari, Carlos Nunez, Maurizio Piai, and James Rucinski. Stability of holographic confinement with magnetic fluxes. *Phys. Rev. D*, 111(6):066009, 2025. doi: 10.1103/PhysRevD.111.066009.

[44] Niko Jokela, Jani Kastikainen, Carlos Nunez, José Manuel Penín, Helime Ruotsalainen, and Javier G. Subils. On entanglement c-functions in confining gauge field theories. *JHEP*, 11:101, 2025. doi: 10.1007/JHEP11(2025)101.

[45] Carlos Nunez and Dibakar Roychowdhury. Timelike entanglement entropy: A top-down approach. *Phys. Rev. D*, 112(2):026030, 2025. doi: 10.1103/vjyt-xc15.

[46] Dimitrios Chatzis, Madison Hammond, Georgios Itsios, Carlos Nunez, and Dimitrios Zoakos. Universal observables, SUSY RG-flows and holography. *JHEP*, 08:134, 2025. doi: 10.1007/JHEP08(2025)134.

[47] Niall T. Macpherson, Paul Merrikin, Carlos Nunez, and Ricardo Stuardo. Twisted-circle compactifications of SQCD-like theories and holography. *JHEP*, 08:146, 2025. doi: 10.1007/JHEP08(2025)146.

[48] Carlos Nunez and Dibakar Roychowdhury. Interpolating between spacelike and timelike entanglement via holography. *Phys. Rev. D*, 112(8):L081902, 2025. doi: 10.1103/x3zd-llsx.

[49] Dimitrios Chatzis, Madison Hammond, Georgios Itsios, Carlos Nunez, and Dimitrios Zoakos. Supersymmetric AdS Solitons, Coulomb Branch Flows and Twisted Compactifications. *arXiv preprint arXiv:2511.18128*, 11 2025.

[50] Ali Fatemiabhari, Horatiu Nastase, Carlos Nunez, and Dibakar Roychowdhury. Holographic Krylov complexity in confining gauge theories. *arXiv preprint arXiv:2511.22717*, 11 2025.

[51] Rhucha Deshpande and Oleg Lunin. Multi-charged geometries with cosmological constant. *JHEP*, 03:131, 2025. doi: 10.1007/JHEP03(2025)131.

[52] E. Cremmer, B. Julia, and Joel Scherk. Supergravity Theory in 11 Dimensions. *Phys. Lett. B*, 76:409–412, 1978. doi: 10.1016/0370-2693(78)90894-8.

[53] Edward Witten. String theory dynamics in various dimensions. *Nucl. Phys. B*, 443:85–126, 1995. doi: 10.1016/0550-3213(95)00158-O.

[54] B. de Wit and H. Nicolai. The Consistency of the S**7 Truncation in D=11 Supergravity. *Nucl. Phys. B*, 281:211–240, 1987. doi: 10.1016/0550-3213(87)90253-7.

[55] B. de Wit and H. Nicolai. N=8 Supergravity. *Nucl. Phys. B*, 208:323, 1982. doi: 10.1016/0550-3213(82)90120-1.

[56] Mirjam Cvetic, M. J. Duff, P. Hoxha, James T. Liu, Hong Lu, J. X. Lu, R. Martinez-Acosta, C. N. Pope, H. Sati, and Tuan A. Tran. Embedding AdS black holes in ten-dimensions and eleven-dimensions. *Nucl. Phys. B*, 558:96–126, 1999. doi: 10.1016/S0550-3213(99)00419-8.

[57] Z. W. Chong, Mirjam Cvetic, H. Lu, and C. N. Pope. General non-extremal rotating black holes in minimal five-dimensional gauged supergravity. *Phys. Rev. Lett.*, 95:161301, 2005. doi: 10.1103/PhysRevLett.95.161301.

[58] Peter Breitenlohner and Daniel Z. Freedman. Positive Energy in anti-De Sitter Backgrounds and Gauged Extended Supergravity. *Phys. Lett. B*, 115:197–201, 1982. doi: 10.1016/0370-2693(82)90643-8.

[59] Andres Anabalon, Dumitru Astefanesei, and Julio Oliva. Hairy Black Hole Stability in AdS, Quantum Mechanics on the Half-Line and Holography. *JHEP*, 10:068, 2015. doi: 10.1007/JHEP10(2015)068.

[60] Andres Anabalon, Dumitru Astefanesei, and Cristian Martinez. Mass of asymptotically anti–de Sitter hairy spacetimes. *Phys. Rev. D*, 91(4):041501, 2015. doi: 10.1103/PhysRevD.91.041501.

[61] Ofer Aharony, Oren Bergman, Daniel Louis Jafferis, and Juan Maldacena. N=6 superconformal Chern-Simons-matter theories, M2-branes and their gravity duals. *JHEP*, 10:091, 2008. doi: 10.1088/1126-6708/2008/10/091.

[62] Werner Israel. Event horizons in static vacuum space-times. *Phys. Rev.*, 164:1776–1779, 1967. doi: 10.1103/PhysRev.164.1776.

[63] B. Carter. Axisymmetric black hole has only two degrees of freedom. *Phys. Rev. Lett.*, 26:331–333, Feb 1971. doi: 10.1103/PhysRevLett.26.331. URL https://link.aps.org/doi/10.1103/PhysRevLett.26.331.

[64] S. W. Hawking. Black holes in general relativity. *Commun. Math. Phys.*, 25:152–166, 1972. doi: 10.1007/BF01877517.

[65] D. C. Robinson. Uniqueness of the Kerr black hole. *Phys. Rev. Lett.*, 34: 905–906, 1975. doi: 10.1103/PhysRevLett.34.905.

[66] Jacob D. Bekenstein. Black holes and entropy. *Phys. Rev. D*, 7:2333–2346, Apr 1973. doi: 10.1103/PhysRevD.7.2333. URL https://link.aps.org/doi/10.1103/PhysRevD.7.2333.

[67] S. W. Hawking. Gravitational radiation from colliding black holes. *Physical Review Letters*, 26(21):1344–1346, 1971. doi: 10.1103/PhysRevLett.26.1344.

[68] Jacob D. Bekenstein. Generalized second law of thermodynamics in black-hole physics. *Phys. Rev. D*, 9:3292–3300, Jun 1974. doi: 10.1103/PhysRevD.9.3292. URL https://link.aps.org/doi/10.1103/PhysRevD.9.3292.

[69] S. W. Hawking. Particle Creation by Black Holes. *Commun. Math. Phys.*, 43:199–220, 1975. doi: 10.1007/BF02345020. [Erratum: Commun.Math.Phys. 46, 206 (1976)].

[70] James M. Bardeen, B. Carter, and S. W. Hawking. The Four laws of black hole mechanics. *Commun. Math. Phys.*, 31:161–170, 1973. doi: 10.1007/BF01645742.

[71] Andrew Chamblin, Roberto Emparan, Clifford V. Johnson, and Robert C. Myers. Charged AdS black holes and catastrophic holography. *Phys. Rev. D*, 60:064018, 1999. doi: 10.1103/PhysRevD.60.064018.

[72] S. W. Hawking, C. J. Hunter, and M. M. Taylor-Robinson. Rotation and the ads-cft correspondence. *Physical Review D*, 59(6), February 1999. ISSN 1089-4918. doi: 10.1103/physrevd.59.064005. URL http://dx.doi.org/10.1103/PhysRevD.59.064005.

[73] Veronika E. Hubeny. The AdS/CFT Correspondence. *Class. Quant. Grav.*, 32(12):124010, 2015. doi: 10.1088/0264-9381/32/12/124010.

[74] L. F. Abbott and Stanley Deser. Stability of Gravity with a Cosmological Constant. *Nucl. Phys. B*, 195:76–96, 1982. doi: 10.1016/0550-3213(82)90049-9.